Spin-orbit coupling and its effects in organic solids

Z. G. Yu

Phys. Rev. B **85**, 115201 — Published 2 March 2012

DOI: 10.1103/PhysRevB.85.115201

Spin-orbit coupling and its effects in organic solids

Z. G. Yu
Physical Sciences Division, SRI International, 333 Ravenswood Avenue, Menlo Park, California 94025, USA
(Dated: February 7, 2012)

We present a detailed analysis of spin-orbit coupling (SOC) in π-conjugated organic materials and its effects on spin characteristics including the spin relaxation time, spin diffusion length, and g factor. While π electrons are responsible for low-energy electrical and optical processes in π-conjugated organic solids, σ electrons must be explicitly included to properly describe the SOC. The SOC mixes up- and down-spin states, and in the context of spintronics, can be quantified by an admixture parameter in the electron and hole polaron states in π-conjugated organics. Molecular geometry fluctuations such as ring torsion, which are common in soft organic materials and may depend on sample preparation, are found to have a strong effect on the spin mixing. The SOC-induced spin mixing leads to spin flips as polarons hop from one molecule to another, giving rise to spin relaxation and diffusion, which are examined by the time-dependent perturbation theory and density-matrix theory. The spin relaxation rate is found to be proportional to the carrier hopping rate, or equivalently, carrier mobility. The spin diffusion length depends on the spin mixing and hopping distance but is insensitive to the carrier mobility. An applied electric field causes spin drift and gives rise to upstream and downstream spin diffusion lengths in the hopping-conduction regime. The SOC influences the g factor of the polaron state and make it deviate from the free-electron value. The deviation is due to the mixing of different *orbitals* in the polaron state, which does not include the spin mixing within a same orbital, and therefore underestimates the SOC strength. In particular, the g factor is not sensitive to the molecular geometry fluctuations, where the spin mixing within a same orbital is dominant. The SOCs in tris-(8-hydroxyquinoline) aluminum (Alq_3) and in copper phthalocyanine (CuPc) are particularly strong, due to the orthogonal arrangement of the three ligands in the former and Cu $3d$ orbitals in the latter. The theory quantitatively explains the recent measured spin diffusion lengths in Alq_3 from muon spin rotation and in CuPc from spin-polarized two-photon photoemission.

PACS numbers: 72.80.Le, 71.70.Ej, 72.25.Rb, 76.30.Pk

I. INTRODUCTION

Organic spintronics combines the advantages of spintronics[1] and low-cost fabrication of organic devices and has advanced rapidly since the discovery of large magnetoresistance in ferromagnet-organic-ferromagnet structures.[2,3] Weak spin-orbit couplings (SOCs) and hyperfine interactions (HFIs) are frequently invoked as one of major virtues of organic spintronics.[4] To date, however, there is little quantification of these interactions in individual organic materials, which prevents direct comparison among different organics and quantitative understanding of spin relaxation and transport in organic materials. While the HFI in an organic material in principle can be directly measured by the nuclear magnetic resonance and electron spin resonance (ESR) experiments, the SOC is not directly measurable and its meaning in the context of organic spintronics is often unclear. Although all organic materials contain the C element, which has a relatively small atomic SOC, many organic materials studied for spintronic applications also contain heavier elements, such as O in poly[2-methoxy-5-(2'-ethylhexyloxy)-*p*-phenylene vinylene] (MEH-PPV), O, N, and Al in tris-(8-hydroxyquinoline) aluminum (Alq_3), S in sexithienyl (T_6), and Cu in copper phthalocyanine (CuPc), which have stronger atomic SOCs, as listed in Table I.[5] There is no systematic way available to estimate different elements' contributions to the total SOC in a given organic. Another complication is that in organic solids the organic molecules or oligomers are usually packed differently because organics are flexible and their geometry strongly fluctuates.[6] To meaningfully compare experiments, one needs to know to what extent the packing or the geometry variation can influence the SOC. Thus a good SOC measure that is relevant to spintronics and can be systematically evaluated in individual organics is acutely needed.

TABLE I: Atomic SOC strengths of common elements in organics.

Element	Orbital	ξ (cm^{-1})
C	$2p$	11
N	$2p$	76
O	$2p$	151
Al	$3p$	112
S	$3p$	382
Cu	$3d$	829

Understanding spin relaxation can help harness the spin degree of freedom effectively in device structures. While spin relaxation in inorganic metals and semiconductors are well understood, thanks largely to the classic and rigorous works by Elliott and Yafet (EY)[7] and D'yakonov and Perel' (DP),[8] very few studies of spin relaxation in organics were carried out, especially relaxation caused by the SOC. Theories developed so far are

usually primitive, inadequate, and sometimes even invalid. Because of the lack of systematic theoretical studies on organics in literature, theories for crystalline inorganic semiconductors and for isolated molecules in the ESR literature[9] have been frequently used to estimate important parameters such as spin lifetimes and spin diffusion lengths in highly disordered organic solids with little justification. Such a casual use of existing theories resulted in wildly inconsistent estimates from different groups. For example, the spin lifetime estimated for Alq_3 ranges from 10^{-6} s to 1 s.[3,10–12] One must keep in mind that EY and DP theories were developed for crystalline semiconductors and the corresponding expressions may not be applicable to the organic materials used in organic spintronic devices, which are dense films of randomly orientated conjugated oligomers or molecules. Nor can the spin relaxation theories of immobile electrons on isolate organic molecules[9,13] be directly applicable to the organic solids, for electrons (or, more precisely, polarons – electrons with local lattice distortions) in the organic solids are mobile. Thus, it is imperative to establish systematic and rigorous theories that consistently describe spin relaxation in organic solids. Experimentally, carrier spin relaxation times (longitudinal T_1 and transverse T_2) in organics can be measured by electrically detected spin resonance.[14]

The spin diffusion length poses a constrain on the channel length of a spintronic device and has recently been directly measured by muon spin rotation in Alq_3[15] and by spin-polarized two-photon photoemission in CuPc.[16] These measurements provide an excellent opportunity to compare theory with experiment. In literature, the formula $L_s = \sqrt{DT_1}$ with L_s and D being the spin diffusion length and carrier diffusion constant, is often used to argue that the spin diffusion length can be greatly enhanced if the carrier mobility is improved. This argument tacitly assumes that D and T_1 are independent of each other, which is questionable, for, fundamentally, the carrier spin relaxation must be closely related to the transport properties of the carriers, such as mobility.[7,8]

In organics devices, the carrier density is usually low and the electric field can be large. The electric field is found to significantly affect spin diffusion and spin injection in inorganic semiconductors.[17] The major difference between inorganic and organic solids is that electrical transport is via band conduction in the former and carrier hopping in the latter. It is interesting to know how the electric field affects spin diffusion length in the hopping regime. This understanding is crucial to describe the device characteristics and to manipulate spin by using the electric field, or equivalently, bias voltage.

HFIs can cause spin relaxation and diffusion as well.[18,19] The HFI implies isotope effects, which are found in PPV[20] but not in Alq_3,[21] indicating that the relative importance of SOC and HFI varies among individual organic materials. Because of their different natures, the SOC and HFI will lead to different temperature and magnetic-field dependences of spin relaxation and diffusion. Therefore it is valuable to establish the corresponding temperature and magnetic-field dependences caused by the SOC and HFI, which can be used to determine the dominant spin-relaxation mechanisms experimentally in individual organics.

The g factors of electron and hole polarons in organic materials are influenced by the SOC and can be measured by ESR.[9] The measured g factor in disordered organic solids is an average over random orientations of oligomers or molecules. Since the g-factor deviation depends on the SOC, it is natural to ask whether the g-factor deviation can be used to adequately characterize the SOC in organics.

Here we present a comprehensive study of the SOC and address all the issues enumerated above. We also compare our theoretical results with relevant experiments in literature whenever possible. Some preliminary results of this work have been reported in a short paper.[22] This article is organized as follows. After the introduction, we study the SOC and evaluate its strengths in various organics in Sec. II. Then we use the perturbation and density-matrix theories and provide rigorous results on spin relaxation in Sec. III and spin diffusion length in Sec. IV. We examine the electric-field effect on spin diffusion in the hopping regime in Sec. V. In Sec. VI, we analyze the g-factor deviation in disordered organic solids due to the SOC. Finally we summarize our results in Sec. VII.

II. SPIN-ORBIT COUPLING IN ORGANICS

In π-conjugated organics the electronic structure is derived from sp^2 hybridization of the C atoms with the sp^2 orbitals forming σ bonds and p_z orbitals forming π bonds. The electrical transport and optical properties are essentially controlled by the π electrons, for σ electrons are several eVs away in energy from the valence electrons. Thus most models for conjugated organics consider only π electrons explicitly, such as the well-known Su-Schrieffer-Heeger model.[23] These π-electron models, however, become inadequate in studying the SOC because, by definition, the SOC allows exchange between orbital and spin angular momenta. By neglecting the σ orbitals, i.e. the p_x and p_y orbitals, the orbital angular momentum is completely quenched and so is the SOC.[24,25] Hence one must explicitly take into account the σ orbitals when studying the SOC in organics. In fact, the σ orbitals are also needed to account for the HFI of the π electrons.[26] Without the σ orbitals, the isotropic HFI of π electrons would be zero.

Similar situation occurs in inorganic semiconductors like GaAs,[27] where the conduction band is formed primarily from the s orbital, which does not have any orbital angular momentum or SOC. The finite SOC of conduction-band electrons comes from the valence band, which is comprised of p orbitals. Just as one cannot confine oneself to the s orbitals in studying the SOC in

semiconductors, one cannot study the SOC from the pure π-electron models in organics.

A. Fictitious atom

For clarity we first consider a fictitious atom in a $2p$ state which is subjected to a potential field that lowers the energy of the p_z orbital relative to p_x and p_y by Δ, mimicking the situation that the σ orbitals have a higher energy than π orbitals. The atomic SOC is $H_{SO} = \xi \boldsymbol{l} \cdot \boldsymbol{s}$. The spin quantization axis is assumed to be along the z-axis and coincide with the p_z orbital. From the perturbation theory, the doubly degenerate eigenstates with the lowest energy are

$$|+\rangle = |p_z \uparrow\rangle + \frac{\xi}{2\Delta}|(p_x + ip_y)\downarrow\rangle, \tag{2.1}$$

$$|-\rangle = |p_z \downarrow\rangle - \frac{\xi}{2\Delta}|(p_x - ip_y)\uparrow\rangle. \tag{2.2}$$

The energy correction due to the SOC, to the second order of ξ, is

$$\delta E = -\frac{\xi^2}{\Delta}. \tag{2.3}$$

The two states remain degenerate as required by the time-reversal symmetry. We see that the SOC mixes up- and down-spin in an eigenstate and renders the spin not a good quantum number. We can define the dimensionless measure of SOC as the admixture of up- and down-spin in an eigenstate,

$$\gamma^2 = \frac{\xi^2}{2\Delta^2}. \tag{2.4}$$

This measure reflects not only the atomic SOC (ξ) but also the π-σ energy splitting Δ. It follows that the larger energy difference between π and σ orbitals, the smaller the effective SOC.

In organic solids experimentally studied, the orientation of individual oligomers or molecules (or, equivalently, orbitals) are random. However, the spin orientation is well defined, determined by either an applied magnetic field or the magnetization of the ferromagnetic electrode. Thus in general, the π orbital in an organic can be oriented along an arbitrary direction (θ_1, ϕ_1) with respect to the spin quantization axis. In this case, the local π orbital, p'_z, and the other two local orbitals can be expressed as linear combinations of the three p orbitals for $(\theta_1, \phi_1) = (0, 0)$,

$$p'_z = \sin\theta_1\cos\phi_1 p_x + \sin\theta_1\sin\phi_1 p_y + \cos\theta_1 p_z, \tag{2.5}$$

$$p'_x = \cos\theta_1\cos\phi_1 p_x + \cos\theta_1\sin\phi_1 p_y - \sin\theta_1 p_z, \tag{2.6}$$

$$p'_y = -\sin\phi_1 p_x + \cos\phi_1 p_y. \tag{2.7}$$

The eigenstates with the lowest energy, after including the SOC, are

$$|+'\rangle = |p'_z \uparrow\rangle + \frac{\xi}{2\Delta}\big[-i\sin\theta_1|p'_y\uparrow\rangle + e^{i\phi_1}|p'_x\downarrow\rangle + i\cos\theta_1 e^{i\phi_1}|p'_y\downarrow\rangle\big], \tag{2.8}$$

$$|-'\rangle = |p'_z \downarrow\rangle + \frac{\xi}{2\Delta}\big[i\sin\theta_1|p'_y\downarrow\rangle e^{-i\phi_1}|p'_x\uparrow\rangle + i\cos\theta_1 e^{-i\phi_1}|p'_y\uparrow\rangle\big]. \tag{2.9}$$

It is readily to verify that $|+'\rangle$ and $|-'\rangle$ are orthogonal, $\langle+'|-'\rangle = 0$. And $\langle+'|+'\rangle = \langle-'|-'\rangle = 1 + \xi^2/2\Delta^2$.

The expectation values of the spin operator $\hat{\sigma}_z$ in these two states are

$$p_+ = \langle+'|\hat{\sigma}_z|+'\rangle = 1 - \frac{\xi^2}{2\Delta^2}\cos^2\theta_1, \tag{2.10}$$

$$p_- = \langle-'|\hat{\sigma}_z|-'\rangle = -\Big(1 - \frac{\xi^2}{2\Delta^2}\cos^2\theta_1\Big). \tag{2.11}$$

In Appendix A, $|+'\rangle$ ($|-'\rangle$) is shown to have the maximal expectation value of $\hat{\sigma}_z$ ($-\hat{\sigma}_z$) in any linear combination of $|+'\rangle$ and $|-'\rangle$, and therefore is the quasi up-spin (down-spin) state.

Again in Eqs. (2.8) and (2.9) the SOC mixes up-spin and down-spin in an eigenstate, and its admixture is

$$\gamma^2_{\uparrow\downarrow} = \Big(\frac{\xi}{2\Delta}\Big)^2\frac{1}{2}\Big[\cos^2\theta_1 + 1\Big]. \tag{2.12}$$

In addition, the SOC also mixes orbitals with a same spin,

$$\gamma^2_{\uparrow\uparrow} = \Big(\frac{\xi}{2\Delta}\Big)^2\frac{1}{2}\sin^2\theta_1. \tag{2.13}$$

Since the SOC is an intrinsic material property, which should not depend on the molecular orientation, a more suitable SOC measure can be constructed as

$$\gamma^2 = \gamma^2_{\uparrow\uparrow} + \gamma^2_{\uparrow\downarrow} = \frac{\xi^2}{2\Delta^2}, \tag{2.14}$$

which is the combination of the orbital mixing and spin mixing and independent of the molecular orientation.

B. First-principles approach for real molecules

Now we consider real organic molecules. In the context of spintronics, it is the carrier or polaron whose

spin-dependent properties really matter. Thus we focus on the highest occupied molecular orbitals (HOMOs) of negatively charge and positively charged molecule or oligomer, which correspond to the electron polaron and hole polaron states. Note the HOMO here is half filled because of the presence of the carrier (polaron) and should not be confused with the completely filled HOMO in an intrinsic molecules. The total Hamiltonian of an organic molecule can be written as

$$H = H_0 + H_{SO} = H_0 + \sum_i \xi_i \boldsymbol{l}_i \cdot \boldsymbol{s}_i, \tag{2.15}$$

where H_0 is the Hamiltonian without the SOC and H_{SO} is the summation of all atomic SOC contributions. Because of the generally weak atomic SOC strengths compared to bonding energies, in most first-principles calculations for organic materials, the SOC is completely neglected and the obtained eigenstates are for $H = H_0$.

In general an eigenstate of H_0, which satisfies $H_0|\psi_k\rangle = E_k|\psi_k\rangle$, can be expressed in terms of the atomic orbitals,

$$|\psi_k\rangle = \sum_{i\alpha} c_{i\alpha}^{(k)} |\phi_i^{(\alpha)}\rangle, \tag{2.16}$$

where k is the index of eigen levels, i is the atom index and α the orbital index, $|\phi_i^{(\alpha)}\rangle$ are atomic orbitals at the ith molecule, and $\phi^{(\alpha)} = 2s, 2p_x, 2p_y, 2p_z$ for O, N, C, $\phi^{(\alpha)} = 1s$ for H, and $\phi^{(\alpha)} = 3s, 3p_x, 3p_y, 3p_z$ for S and Al. These atomic orbitals are not orthogonal with one another and the normalization condition is

$$\sum_{i\alpha}\sum_{j\alpha'} c_{i\alpha}^{(k)} c_{j\alpha'}^{(k)} S_{ij}^{(\alpha\alpha')} = \delta_{kk'}, \tag{2.17}$$

where

$$S_{ij}^{(\alpha\alpha')} = \langle \phi_i^{(\alpha)} | \phi_j^{(\alpha')} \rangle \tag{2.18}$$

is the overlap integral between atomic orbitals.

Once the H_{SO} is included, for the HOMO, denoted as $|\psi_0\rangle$, the eigenstate for the quasi up-spin, according to the perturbation theory, is

$$\begin{aligned} |\psi_0+\rangle &= |\psi_0\uparrow\rangle - \sum_{k\neq 0\sigma} \frac{\langle\psi_k\sigma|\sum_i \xi_i \boldsymbol{l}_i\cdot\boldsymbol{s}_i|\psi_0\uparrow\rangle}{E_k - E_0}|\psi_k\sigma\rangle \\ &= |\psi_0,\uparrow\rangle - \frac{1}{2}\sum_{k\neq 0}\frac{\langle\psi_k|\sum_i \xi_i l_{iz}|\psi_0\rangle}{E_k-E_0}|\psi_k\uparrow\rangle - \frac{1}{2}\sum_{k\neq 0}\frac{\langle\psi_k|\sum_i \xi_i (l_{ix}+il_{iy})|\psi_0\rangle}{E_k-E_0}|\psi_k\downarrow\rangle. \end{aligned} \tag{2.19}$$

Similarly, the eigenstate for the quasi down-spin is

$$|\psi_0-\rangle = |\psi_0\downarrow\rangle + \frac{1}{2}\sum_{k\neq 0}\frac{\langle\psi_k|\sum_i \xi_i l_{iz}|\psi_0\rangle}{E_k-E_0}|\psi_k\downarrow\rangle - \frac{1}{2}\sum_{k\neq 0}\frac{\langle\psi_k|\sum_i \xi_i (l_{ix}-il_{iy})|\psi_0\rangle}{E_k-E_0}|\psi_k\uparrow\rangle. \tag{2.20}$$

Using the relation $\hat{l}_{iq}p_r^i = i\epsilon_{qrs}p_s^i$, where $\hat{l}_{iq}$ is the q component of the angular momentum operator for the ith atom and ϵ_{qrs} is antisymmetric unit tensor of rank three, we can express the HOMO level as

$$|\psi_0+\rangle = |\psi_0\uparrow\rangle + \sum_{i\alpha}\left[a_{i\alpha}|\phi_i^{(\alpha)}\uparrow\rangle + b_{i\alpha}|\phi_i^{(\alpha)}\downarrow\rangle\right], \tag{2.21}$$

and the spin admixture can be computed via

$$\gamma^2 = \gamma_{\uparrow\uparrow}^2 + \gamma_{\uparrow\downarrow}^2 \equiv \sum_{ij}(a_{i\alpha}^* a_{j\alpha'} + b_{i\alpha}^* b_{j\alpha'})S_{ij}^{(\alpha\alpha')}. \tag{2.22}$$

To verify the validity of the above approach, we consider a benzene molecule and use SIESTA,[28] which will be employed to perform first-principles calculations throughout this paper, to obtain all $|\psi_k\rangle$. We fix the spin quantization axis along the z-axis and rotate the benzene molecule with respect to the C_3-C_6 axis. Figure 1 plots $\gamma_{\uparrow\uparrow}^2$ and $\gamma_{\uparrow\downarrow}^2$ for the HOMO in both negatively and positively charged benzene as a function of the rotation angle θ. We see that $\gamma_{\uparrow\downarrow}^2$ and $\gamma_{\uparrow\uparrow}^2$ vary with θ approximately as $\sim(\cos^2\theta+1)/2$ and $\sim\sin^2\theta$. The summation, however, is a constant and independent of θ. Thus spin admixture γ^2 can be reliably evaluated from first-principles approaches.

C. CuPc

Some π-conjugated organics studied for organic spintronics contain transition-metal ions, whose d electrons can have a very strong SOC. One representative example is copper phthalocyanine (CuPc), where the valence of Cu is 2^+ and the electron configuration is $3d^9$. To

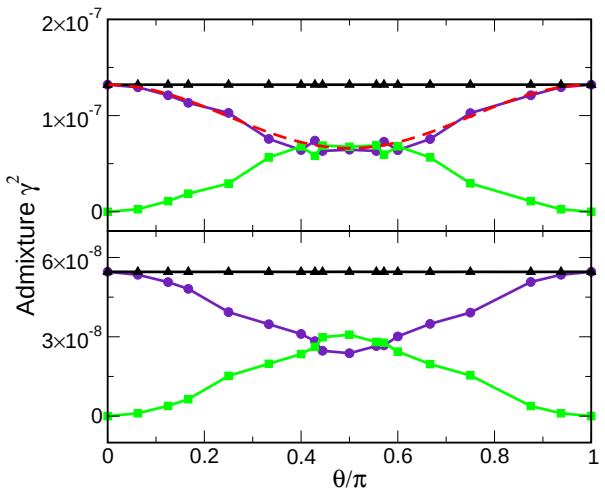

FIG. 1: (color online) Spin admixture γ^2 as a function of θ for the electron (upper panel) and hole (lower panel) polarons in benzene. Circles and squares are the spin-mixing and orbital-mixing contributions, $\gamma^2_{\uparrow\downarrow}$ and $\gamma^2_{\uparrow\uparrow}$, respectively. Triangles are the summation of the two contributions. The dashed line in the upper panel plots the function of $\gamma^2(1+\cos^2\theta)/2$.

account for strong electron correlations in the $3d$ orbitals, sophisticated corrections must be included in first-principles calculations, which inevitably obscure the discussion of the spin mixing. Instead, we use the ligand-field theory[29] to evaluate spin admixture γ^2 in CuPc.

CuPc has a planar structure (shown in Fig. 2), which can be regarded as a cubic structure with a very strong tetragonal distortion. For a strong ligand such as phthalocyanine, in a cubic structure, the 5-fold degenerate $3d$ orbital splits into a 3-fold degenerate t_{2g} orbital and a 2-fold degenerate e_g orbital. Under a tetragonal distortion, the e_g orbitals further split, with $d_{x^2-y^2}$ having a higher energy than d_{z^2}. This situation is very similar to that of high-T_c superconducting copper oxides.

The $3d^9$ configuration means a hole in the $d_{x^2-y^2}$ or E'' orbital. Since the SOC couples $3d$ orbitals with different magnetic quantum numbers, the polaron states at $d_{x^2-y^2}$, after taking into account the SOC, become

$$|E''+\rangle = |d_{x^2-y^2}\uparrow\rangle + \frac{i\xi_{\rm Cu}}{\Delta_1}|d_{xy}\uparrow\rangle + \frac{\xi_{\rm Cu}}{\sqrt{2}\Delta_2}|-1\downarrow\rangle, \quad (2.23)$$

$$|E''-\rangle = |d_{x^2-y^2}\downarrow\rangle - \frac{i\xi_{\rm Cu}}{\Delta_1}|d_{xy}\downarrow\rangle + \frac{\xi_{\rm Cu}}{\sqrt{2}\Delta_2}|1\uparrow\rangle. \quad (2.24)$$

Here Δ_1 and Δ_2 are the energy differences between $3d_{x^2-y^2}$ and $3d_{xy}$ and between $3d_{x^2-y^2}$ and $3d_{yz}$. As shown in Fig. 2, $3d_{xy}$ and $3d_{yz}$ have slightly different energies. $|1\rangle$ and $|-1\rangle$ are $3d$ orbitals with magnetic quantum number of 1 and -1,

$$|1\rangle = -\frac{1}{\sqrt{2}}(d_{zx}+id_{yz}),\ |-1\rangle = \frac{1}{\sqrt{2}}(d_{zx}-id_{yz}). \quad (2.25)$$

The covalence bonding between the Cu^{2+} ion and four central N atoms in phthalocyanine in CuPc delocalizes the wave function of an eigenstate from the Cu ion over to the ligand,

$$d_{x^2-y^2} \to \eta d_{x^2-y^2} + \frac{1}{2}\sqrt{1-\eta^2}(\sigma_1-\sigma_2+\sigma_3-\sigma_4). \quad (2.26)$$

where σ_i $(i=1,2,3,4)$ is the atomic orbital of ith N atom and the linear combination of σ_i in the parenthesis has the same symmetry as the $d_{x^2-y^2}$ orbital. Here parameter η measures how much the electron wave function spreads into the N atoms due to the covalence bonding: the closer η to 1, the more confined the wave function to the Cu ion. Since the atomic SOC of N is negligible compared to that of Cu, the bonding between Cu^{2+} and the ligand leads to an effective SOC in CuPc,

$$\tilde{\xi}_{\rm Cu} = \eta^2\xi_{\rm Cu}. \quad (2.27)$$

The spin admixture in $|E''\rangle$, with the covalence bonding included, is

$$\gamma^2 = \left(\frac{\tilde{\xi}_{\rm Cu}}{\Delta_1}\right)^2 + \frac{1}{2}\left(\frac{\tilde{\xi}_{\rm Cu}}{\Delta_2}\right)^2. \quad (2.28)$$

According to literature,[30] $\Delta_1 = 31,700$ cm^{-1}, $\Delta_2 = 29,000$ cm^{-1}, and $\eta^2 = 0.79$. Using these values, we obtain the spin admixture parameter in CuPc $\gamma^2 = 6.8\times10^{-4}$.

When the normal of the CuPc plane is tilted at $(\theta,\,\phi)$ with respect to the spin quantization axis, the quasi up- and down-spin states become

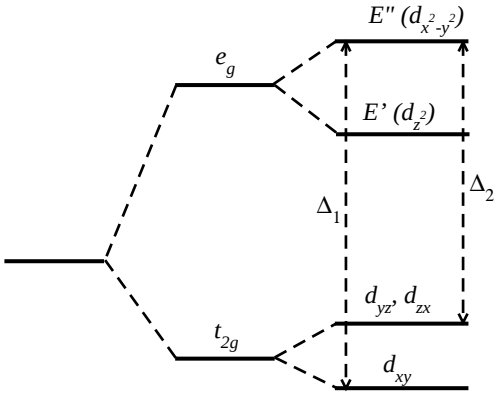

FIG. 2: Molecular structure of CuPc and orbital pattern for a single d electron in a field of tetragonal symmetry.

$$
\begin{aligned}
|E''+\rangle &= |d_{x^2-y^2}\uparrow\rangle + \frac{\tilde{\xi}_{\rm Cu}}{\Delta_1}\Big(i\cos\theta|d_{xy}\uparrow\rangle + i\sin\theta e^{i\phi}|d_{xy}\downarrow\rangle\Big) \\
&+ \frac{1}{2\sqrt{2}}\frac{\xi_{\rm Cu}}{\Delta_2}\Big(-\sin\theta|-1\uparrow\rangle - \sin\theta|1\uparrow\rangle \\
&+ (1+\cos\theta)e^{i\phi}|-1\downarrow\rangle - (1-\cos\theta)e^{i\phi}|1\downarrow\rangle\Big), \qquad (2.29)
\end{aligned}
$$

$$
\begin{aligned}
|E''-\rangle &= |d_{x^2-y^2}\downarrow\rangle + \frac{\tilde{\xi}_{\rm Cu}}{\Delta_1}\Big(-i\cos\theta|d_{xy}\downarrow\rangle + i\sin\theta e^{-i\phi}|d_{xy}\uparrow\rangle\Big) \\
&+ \frac{1}{2\sqrt{2}}\frac{\xi_{\rm Cu}}{\Delta_2}\Big(\sin\theta|-1\downarrow\rangle + \sin\theta|1\downarrow\rangle \\
&+ (1+\cos\theta)e^{-i\phi}|1\uparrow\rangle - (1-\cos\theta)e^{-i\phi}|-1\uparrow\rangle\Big). \qquad (2.30)
\end{aligned}
$$

It is readily verified that the spin admixture for $|E''\pm\rangle$ in Eqs. (2.29) and (2.30), after including both the spin and orbital mixings, is identical to that given by Eq. (2.28). These wave functions will be used to evaluate spin-conserving and spin-flip hopping rates in Sec. IV.

D. Effect of molecular geometry

Simple π-conjugated organics tend to form planar structures, such as benzene and polyacetylene. In complex organic molecules, however, geometry hindrance and bonding constrains can make the structure non-planar. In addition, organic materials are flexible and the relative orientation between different parts in a molecule can fluctuate. To capture the essence of this seemingly tedious effect, we consider two simple cases. One is a molecule consisting of the two fictitious atoms introduced in Sec. II.A; and the other is a twisted biphenyl. In the former, the p_x orbitals of the two atoms are assumed to be parallel and forming a σ bond, and the π overlaps between p_y and p_z orbitals in the two atoms depend on the orientation around the σ bond. In the latter, there is a torsion angle between the two phenyl rings in biphenyl.

For the molecule consisting of two fictitious atoms, the Hamiltonian reads

$$H = H_0 + H_{SO} + H_t, \tag{2.31}$$

where H_0 includes orbital energies and the σ-bonding the coupling between p'_x and p''_x of the two atoms, H_{SO} is the SOC in the two atoms,

$$H_{SO} = \xi(\boldsymbol{l}_1 \cdot \boldsymbol{s}_1 + \boldsymbol{l}_2 \cdot \boldsymbol{s}_2), \tag{2.32}$$

and H_t is the spin-independent π-π coupling

$$\begin{aligned} H_t = \Big[& t_\pi \cos(\theta_2 - \theta_1)(|p'_z\uparrow\rangle\langle p''_z\uparrow| + |p'_y\uparrow\rangle\langle p''_y\uparrow|) \\ + \; & t_\pi \sin(\theta_2 - \theta_1)(|p'_y\uparrow\rangle\langle p''_z\uparrow| - |p'_z\uparrow\rangle\langle p''_y\uparrow|) \\ + \; & \text{H.c.} + (\downarrow\rightarrow\uparrow)\Big]. \end{aligned} \tag{2.33}$$

Here we have used p'_q (p''_q) ($q = x, y, z$) to represent orbitals in the first (second) atom. If we consider $H_0 + H_{SO}$ as the unperturbed Hamiltonian and H_t as a perturbation, the zeroth-order wave functions are $|\pm'\rangle$ and $|\pm''\rangle$ introduced in Eqs. (2.8) and (2.9). Because of the spatial symmetry, we construct the basis set based on the even or odd parity,

$$|E_\pm\rangle = \frac{1}{\sqrt{2}}(|\pm'\rangle + |\pm''\rangle), \tag{2.34}$$

$$|O_\pm\rangle = \frac{1}{\sqrt{2}}(|\pm'\rangle - |\pm''\rangle). \tag{2.35}$$

The nonzero matrix elements of H_t between these basis functions are

$$\langle E_+|H_t|E_+\rangle = \langle E_-|H_t|E_-\rangle = t_\pi \cos(\theta_1 - \theta_2), \tag{2.36}$$

$$\begin{aligned} \langle O_+|H_t|O_+\rangle &= \langle O_-|H_t|O_-\rangle \\ &= -t_\pi \cos(\theta_1 - \theta_2), \end{aligned} \tag{2.37}$$

$$\begin{aligned} \langle E_+|H_t|O_-\rangle &= -\langle E_-|H|O_+\rangle \\ &= \frac{\xi t_\pi}{2\Delta} \sin(\theta_2 - \theta_1). \end{aligned} \tag{2.38}$$

The nonzero matrix element of $\langle E_+|H_t|O_-\rangle$ is due to the SOC-induced spin mixing. The eigenstate of the system with the quasi up-spin is

$$\begin{aligned} |\tilde{+}\rangle &= |E_+\rangle - \frac{\xi}{4\Delta}\tan(\theta_2 - \theta_1)|O_-\rangle \\ &= \frac{1}{\sqrt{2}}(|p'_z\uparrow\rangle + |p''_z\uparrow\rangle) + \frac{\xi}{2\sqrt{2}\Delta}\Big[(-i\sin\theta_1|p'_y\uparrow\rangle - i\sin\theta_2|p''_y\uparrow\rangle) + (e^{i\phi_1}|p'_x\downarrow\rangle + e^{i\phi_2}|p''_x\downarrow\rangle) \\ &+ (i\cos\theta_1 e^{i\phi_1}|p'_y\downarrow\rangle + i\cos\theta_2 e^{i\phi_2}|p''_y\downarrow\rangle) - \frac{\tan(\theta_2 - \theta_1)}{2}(|p'_z\downarrow\rangle - |p''_z\downarrow\rangle)\Big], \end{aligned} \tag{2.39}$$

and the spin admixture is

$$\gamma^2 = \frac{\xi^2}{2\Delta^2}[1 + \frac{1}{8}\tan^2(\theta_2 - \theta_1)]. \tag{2.40}$$

This expression suggests that the SOC is greatly enhanced when the two atoms have different orientations and π orbitals are not aligned. We notice that the term proportional to $\tan^2(\theta_1 - \theta_2)$ originates from spin mixing within same orbitals, p'_z and p''_z.

We carry out a first-principles calculation as described in Sec. II.B on biphenyl and display γ^2 as a function of the torsion angle $\theta \equiv \theta_2 - \theta_1$ between the two phenyl rings in Fig. 3. We see a strong enhancement of γ^2 as the torsion angle increases, particularly when the angle is near $\pi/2$, where a "singularity" in the SOC seems to occur as indicated by Eq. (2.39).

We calculate the spin admixture parameter γ^2 of electron and hole polarons in representative organic materials and list the obtained values in Table II.[31] The molecular geometry of the polaron states is optimized in the calculations. Among these organics, benzene, rubrene, poly(*p*-phenylene) (PPP), and C_{60} contain only C (and H). Others contain additional elements: polyaniline (PANI) and polypyrrole (PPy) have N; T_6 has S; MEH-PPV has O; Alq_3 has N, O, and Al; CuPc has Cu and N; N,N'-bis(n-hepta uorobutyl)-3,4:9,10-perylene tetracarboxylic diimide (PTCDI-C4F7), a newly synthesized organic with a high electron mobility,[32] has N, O, and F. The explicit wave functions of Eq. (2.21) for the polaron states allow us to determine contributions from individual atoms to the total SOC. The SOC in Alq_3 is particularly strong, even larger than T_6 and CuPc, which is due mainly to the orthogonal arrangement of three ligands, as in the case of biphenyl. This geometry effect also results in a large SOC in C_{60}, where π orbitals in the 60 C atoms on a sphere cannot maintain a parallel alignment with one another. The strong geometry dependence of the SOC suggests that material morphology and growth condition may lead to very different SOC strengths in nominally identical organic solids.

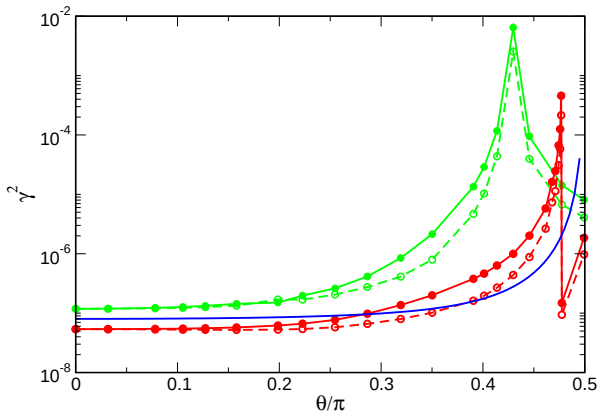

FIG. 3: (color online) Admixture γ^2 as a function of torsion angle θ between the two phenyl rings in biphenyl. Green (light gray) and red (dark gray) circles are for the electron and hole polarons, respectively. Filled circles describe the total spin admixture and open circles describe the spin-mixting contribution. The smooth line is the analytical result from Eq. (2.40).

TABLE II: Spin admixture γ^2 of the electron and hole polarons in representative organics.

Material	Electron polaron	Hole polaron
benzene	1.32×10^{-7}	5.46×10^{-8}
Alq_3	1.07×10^{-3}	7.33×10^{-5}
MEH-PPV	2.64×10^{-7}	3.73×10^{-6}
T_6	4.54×10^{-5}	2.53×10^{-6}
rubrene	1.06×10^{-7}	1.02×10^{-7}
PANI	1.34×10^{-7}	2.84×10^{-7}
PPP	1.20×10^{-7}	6.61×10^{-8}
C_{60}	1.12×10^{-6}	1.31×10^{-6}
CuPc	6.80×10^{-4}	6.80×10^{-4}
PTCDIC4F7	3.59×10^{-6}	1.63×10^{-5}
PPy	6.80×10^{-7}	7.61×10^{-8}

III. SPIN RELAXATION CAUSED BY SOC

Spin relaxation describes an irreversible decay of spin polarization due to chaotic environmental fluctuations and limits the operation speed of a spintronic device. Spin relaxation usually is characterized by two lifetimes, T_1 and T_2, or the longitudinal and transverse spin lifetimes, which are introduced phenomenologically in the Bloch Equation,[9]

$$\frac{d\boldsymbol{S}}{dt} = g\mu_B \boldsymbol{S}\times\boldsymbol{H}_0 - \frac{S_x\boldsymbol{e}_x + S_y\boldsymbol{e}_y}{T_2} - \frac{S_z - S_0}{T_1}\boldsymbol{e}_z, \quad (3.1)$$

where $\boldsymbol{H}_0$ is the applied magnetic field, S_0 is the equilibrium value of $\boldsymbol{S}$, and $\boldsymbol{e}_q$ $(q = x, y, z)$ is the unit vectors along the q-axis. For carriers in organic solids, as we will show later, the two spin relaxation times generally are equal. In this paper, we focus on carrier (mobile electron) spin relaxation caused by the SOC in disordered organic systems where electrical transport is due to polaron hopping, for the materials used for organic spintronics are usually in the form of dense film. We emphasize that the existing spin relaxation theories for crystalline solids[7,8] and for isolated molecule[9,13] are not directly applicable to this situation.

A. Spin-flip and spin-conserving hoppings

The polaron hopping in organic solids in the presence of the SOC can be symbolically expressed by the following Hamiltonian,

$$H = H_0 + H_{SO} + V = \sum_{is} E_i a_{is}^\dagger a_{is} + H_{SO} + \sum_{ijs}\langle j|V|i\rangle a_{js}^\dagger a_{is}. \quad (3.2)$$

Here E_i is the polaron energy at site i and $\langle j|V|i\rangle$ is the hopping integral from site i to site j facilitated by the electron-lattice interaction. Both E_i and $\langle j|V|i\rangle$ are independent of spin, $s = \uparrow, \downarrow$. To elucidate the effect of H_{SO} on the hopping process, we first consider hopping between the two molecules with orientations (θ_1, ϕ_1) and (θ_2, ϕ_2). The polaron eigenstates of $H_0 + H_{SO}$ are $|\pm'\rangle$ at site 1 and $|\pm''\rangle$ at site 2. Since the "up"-spin polaron eigenstate $|+'\rangle$ contains a small down-spin component, the hopping from the polaron eigenstate for spin-up $|+'\rangle$ to the eigenstate for spin-down $|-''\rangle$ is finite even though the polaron hopping Hamiltonian V is spin-independent. We display all four hopping matrix elements between $|\pm'\rangle$ and $|\pm''\rangle$,

$$V_{+''+'} = \langle p_z''|V|p_z'\rangle - \frac{i\xi}{2\Delta}\Big(\cos\theta_1\langle p_z''|V|p_y'\rangle - \sin\theta_2\langle p_y''|V|p_z'\rangle\Big), \quad (3.3)$$

$$V_{-''-'} = \langle p_z''|V|p_z'\rangle + \frac{i\xi}{2\Delta}\Big(\cos\theta_1\langle p_z''|V|p_y'\rangle - \sin\theta_2\langle p_y''|V|p_z'\rangle\Big), \quad (3.4)$$

$$V_{-''+'} = \frac{\xi}{2\Delta}\Big(ie^{i\phi_1}\cos\theta_1\langle p_z''|V|p_y'\rangle - ie^{i\phi_2}\cos\theta_2\langle p_y''|V|p_z'\rangle + e^{i\phi_1}\langle p_z''|V|p_x'\rangle + e^{i\phi_2}\langle p_x''|V|p_z'\rangle\Big), \quad (3.5)$$

$$V_{+''-'} = \frac{\xi}{2\Delta}\Big(-ie^{-i\phi_1}\cos\theta_1\langle p_z''|V|p_y'\rangle + ie^{-i\phi_2}\cos\theta_2\langle p_y''|V|p_z'\rangle + e^{-i\phi_1}\langle p_z''|V|p_x'\rangle + e^{-i\phi_2}\langle p_x''|V|p_z'\rangle\Big). \quad (3.6)$$

Here p'_q and p''_q ($q = x, y, z$) are the local p orbitals in the first and second atoms and their expressions are displayed in Eqs. (2.5)-(2.7) with corresponding (θ_i, ϕ_i) $(i = 1, 2)$. These four complex matrix elements can be described by a spin-independent scalar, V_0, and a real vector $\boldsymbol{V} = (V_x, V_y, V_z)^T$,

$$\begin{pmatrix} V_{+''+'} & V_{+''-'} \\ V_{-''+'} & V_{-''-'} \end{pmatrix} = V_0\hat{1} + \sum_q \hat{\sigma}_q V_q, \tag{3.7}$$

where $\hat{\sigma}_q$ is the Pauli's matrix. If we assume that when the two molecules are aligned, $(\theta_1, \phi_1) = (\theta_2, \phi_2) = (0, 0)$, hopping takes place only between same orbitals, $\langle p''_q|V|p'_{q'}\rangle = v_0\delta_{qq'}$, for randomly orientated molecules, the spin-conserving hopping, after averaging over the molecular orientation, is

$$\overline{V_0^2} = \frac{1}{3}v_0^2. \tag{3.8}$$

And the averaged spin-dependent components are

$$\overline{V_x^2} = \overline{V_y^2} = \overline{V_z^2} = \Big(\frac{\xi}{2\Delta}\Big)^2\frac{4}{9}v_0^2. \tag{3.9}$$

By defining χ_q^2 as

$$\chi_q^2 = \frac{\overline{V_q^2}}{\overline{V_0^2}} = \frac{2}{3}\gamma^2 \equiv \chi^2, \tag{3.10}$$

the ratio between spin-flip hopping rate to spin-conserving one is

$$\frac{w^{+-}}{w^0} = \frac{\overline{|V_{-''+'}|^2}}{\overline{|V_{+''+'}|^2}} = \chi_x^2 + \chi_y^2 = \frac{4}{3}\gamma^2, \tag{3.11}$$

which, as shown in Appendix B, is invariant under any SU(2) rotation. Thus each polaron hop involves a small probability of spin flip, which is characterized by the spin admixture parameter γ^2.

B. Two-site system: Time-dependent perturbation theory

To demonstrate that the spin flip discussed above is indeed related to spin relaxation, we consider hopping from site 1 to site 2 using the time-dependent perturbation theory. In this two-site system, the time-dependent wavefunction can be written as a sum

$$|\Psi(t)\rangle = \sum_{k=1}^{4} a_k(t)e^{-i\omega_k t}|k\rangle, \tag{3.12}$$

where $|1(2)\rangle = |+'(-')\rangle$, $|3(4)\rangle = |+''(-'')\rangle$, and $\hbar\omega_k$ is the polaron energy of $|k\rangle$. The time-dependent coefficient $a_k(t)$ satisfies the following equation[33]

$$i\hbar\frac{da_k}{dt} = \sum_m V_{km}(t)a_m, \tag{3.13}$$

where $V_{km}(t) = V_{km}e^{i\omega_{km}t}$ with V_{km} being the hopping matrix element, $V_{km} = \langle k|V|m\rangle$ and $\omega_{km} = \omega_k - \omega_m$. The nonzero V_{km} are $V_{31} = V_{13}^* = V_{+''+'}$, $V_{42} = V_{24}^* = V_{-''-'}$, $V_{41} = V_{41}^* = V_{-''+'}$, and $V_{32} = V_{23}^* = V_{+''-'}$.

Suppose, at $t = 0$, the electron is at state $|+'\rangle$, i.e., $a_1^{(0)} = 1$ and $a_k^{(0)} = 0$ for $k \neq 1$. Integrating the above equations, we obtain

$$a_1(t) = a_1^{(0)} = 1,\ a_2(t) = a_2^{(0)} = 0, \tag{3.14}$$

$$a_3(t) = a_3^{(1)}(t) = -V_{+''+'}\frac{e^{i\omega t} - 1}{\hbar\omega}, \tag{3.15}$$

$$a_4(t) = a_4^{(1)}(t) = -V_{-''+'}\frac{e^{i\omega t} - 1}{\hbar\omega}, \tag{3.16}$$

where $\hbar\omega$ is the polaron-energy difference between sites 2 and 1.

The expectation values of spin at $t = 0$ and t are

$$s_z(0) = \frac{1}{2}\frac{\langle+'|\sigma_z|+'\rangle}{\langle+'|+'\rangle} = \frac{1 - \frac{\xi^2}{2\Delta^2}\cos^2\theta_1}{2\Big(1 + \frac{\xi^2}{2\Delta^2}\Big)}, \tag{3.17}$$

$$s_z(t) = \frac{1}{2}\frac{\langle\Psi(t)|\sigma_z|\Psi(t)\rangle}{\langle\Psi(t)|\Psi(t)\rangle} = \frac{1 - \frac{\xi^2}{2\Delta^2}\cos^2\theta_1 + \Big(|a_3(t)|^2 - |a_4^2(t)|^2\Big)\Big(1 - \frac{\xi^2}{2\Delta^2}\cos^2\theta_2\Big) + C}{2\Big(1 + |a_3(t)|^2 + |a_4(t)|^2\Big)\Big(1 + \frac{\xi^2}{2\Delta^2}\Big)}, \tag{3.18}$$

where

$$C = -\frac{\xi^2}{2\Delta^2}\sin\theta_2\cos\theta_2\Big(a_3^*(t)a_4(t)e^{i\phi_2} + a_4^*(t)a_3(t)e^{-i\phi_2}\Big). \tag{3.19}$$

The change in spin, $\Delta s_z \equiv s_z(t) - s_z(0)$, due to the polaron hopping is

$$\Delta s_z(t) = \frac{|a_3(t)|^2 \frac{\xi^2}{2\Delta^2}(\cos^2\theta_1 - \cos^2\theta_2) - |a_4(t)|^2\Big[2 - \frac{\xi^2}{2\Delta^2}(\cos^2\theta_1 + \cos^2\theta_2)\Big] + C}{2\Big(1 + |a_3(t)|^2 + |a_4(t)|^2\Big)\Big(1 + \frac{\xi^2}{2\Delta^2}\Big)}. \tag{3.20}$$

Now we examine individual terms in Eq. (3.20). First the cross term C is negligible because 1) it is in third order of ξ/Δ; 2) $\langle +'|V|+\rangle$ and $\langle -'|V|+'\rangle$ can have an arbitrary phase difference and the time average over their product will become zero; 3) it is averaged to be zero over the molecular orientation (θ_2, ϕ_2). The term proportional of $|a_3(t)|^2$ in the numerator is also zero after averaging the relative angle between sites 1 and 2. Hence, to the second order of ξ/Δ,

$$\Delta s_z(t) = -\frac{|a_4(t)|^2}{1 + |a_3(t)|^2 + |a_4(t)|^2} \simeq -|a_4(t)|^2, \tag{3.21}$$

where we have used $|a_3(t)| \ll 1$ and $|a_4(t)| \ll 1$, as required by the validity of perturbation theory. Using the relation $\lim_{t\to\infty} \sin^2\omega t/\pi t\omega^2 = \delta(\omega)$ together with Eq. (3.16), we obtain the spin relaxation rate in this two-site system as

$$-\frac{d\Delta s_z}{dt} = \frac{d|a_4(t)|^2}{dt} = \frac{2\pi}{\hbar}|V_{-''+'}|^2\delta(\omega), \tag{3.22}$$

which is identical to the spin-flip rate w^{+-} introduced earlier. This indicates that spin mixing indeed reduces the expectation value of spin as a polaron hops. In the above example, the initial state has a pure up-spin and therefore only spin flip from up to down, w^{+-}, contributes to spin relaxation. Spin flip from down to up, w^{-+}, will also contributes to spin relaxation if the initial state contains down-spin component, which will be automatically included in a more general density-matrix theory developed in Sec. III.D.

C. Fluctuating-magnetic field approach

Spin relaxation in the ESR literature is often formulated by regarding the environmental fluctuation as a time-dependent magnetic field, under which the spin dynamics is described by the following equation,

$$\frac{d\boldsymbol{S}}{dt} = \frac{g\mu_B}{\hbar}\boldsymbol{S} \times [\boldsymbol{H}_0 + \boldsymbol{h}(t)], \tag{3.23}$$

where $\boldsymbol{H}_0$ is the applied external field and $\boldsymbol{h}(t)$ is a fluctuating field. The fluctuating field has a temporal correlation time τ_c, beyond which the fluctuations are considered unrelated,[9]

$$\overline{h_p(t+\tau)h_q(t)} = \delta_{pq}\overline{h_q^2}e^{-|\tau|/\tau_c}. \tag{3.24}$$

Based on the perturbation theory, the spin relaxation lifetimes T_1 and T_2 are

$$\frac{1}{T_1} = \Big(\frac{g\mu_B}{\hbar}\Big)^2\Big(\overline{h_x^2} + \overline{h_y^2}\Big)\frac{\tau_c}{1 + \omega_0^2\tau_c^2}, \tag{3.25}$$

$$\frac{1}{T_2} = \Big(\frac{g\mu_B}{\hbar}\Big)^2\Big[\tau_c\overline{h_z^2} + \frac{1}{2}\Big(\overline{h_x^2} + \overline{h_x^2}\Big)\frac{\tau_c}{1 + \omega_0^2\tau_c^2}\Big], \tag{3.26}$$

where $\hbar\omega_0 = g\mu_B H_0$ is the Zeeman energy.

Here we show that this approach can also be used in the situation of spin relaxation of polarons. If the reference system is chosen such that the mobile polaron is at rest, the polaron hopping between different sites can be regraded as a temporal variation of the environment, or a local magnetic field h_q,

$$g\mu_B h_q = V_q, \tag{3.27}$$

and for $\omega_0\tau_c \ll 1$, which is usually satisfied in organics because their small τ_c. According to Eqs. (3.25) and (3.26),

$$\frac{1}{T_1} = \frac{1}{T_2} = \frac{1}{\hbar^2}\big(\overline{|V_x|^2} + \overline{|V_y|^2}\big)\tau_c. \tag{3.28}$$

We emphasize that $1/\tau_c$ is not the hopping rate, although they are related. Since hopping can be considered as a tunneling process between the two polaron states, which is large when the two states are in-phase, or correlated, over a long period time. This can be seen from the Fermi Golden rule,

$$w^0 = \frac{2\pi}{\hbar}\overline{|\langle p_z''|V|p_z'\rangle|^2}\rho(E), \tag{3.29}$$

where $\rho(E)$ represents the density of states in the final state, which, after taking into account energy broadening due to the finite correlation time, is

$$\rho(E) = \frac{\hbar\tau_c^{-1}}{\pi}\frac{1}{E^2 + (\hbar\tau_c^{-1})^2}, \tag{3.30}$$

where E is the energy difference between the initial and final states. For $E \ll \hbar/\tau_c$,

$$w^0 = \frac{2}{\hbar^2}\overline{|\langle p_z''|V|p_z'\rangle|^2}\tau_c. \tag{3.31}$$

By substituting τ_c in Eq. (3.28) with Eqs. (3.31), the spin relaxation time is

$$\frac{1}{T_1} = \frac{1}{T_2} = \frac{8}{3}\gamma^2 w^0 = w_{+-} + w_{-+}. \tag{3.32}$$

Again the spin relaxation rate is proportional to hopping rate w^0 and spin admixture parameter γ^2.

D. Density-matrix theory

Spin relaxation can be more rigorously discussed by using the density-matrix theory. The hopping among polaron eigenstates at different sites can be written as $\hat{V} = \sum_{ij} \hat{V}_{ij}$, where

$$\hat{V}_{ij} \equiv \langle i \pm |V| j \pm \rangle = V_{ij}^0 \hat{1} + \sum_q \hat{\sigma}_q V_{ij}^q. \tag{3.33}$$

The spin-polarized carrier density can be expressed in a similar form, $\hat{\rho} = \sum_i \hat{\rho}_i$ with $\hat{\rho}_i = \rho_i^0 \hat{1} + \sum_q \hat{\sigma}_q \rho_i^q$, ρ_i^0 the equilibrium up- or down-spin carrier density in the absence of spin polarization, and ρ_i^q magnetization at site i. The density matrix obeys the following Redfield equation in the interaction representation[9],

$$\frac{d\hat{\rho}}{dt} = -\frac{i}{\hbar}[\hat{V}(t), \hat{\rho}(0)] - \frac{1}{\hbar^2}\int_0^\infty d\tau \overline{[\hat{V}(t), [\hat{V}(t-\tau), \hat{\rho}(0)]]}, \tag{3.34}$$

where $\hat{\rho}(0)$ is the density matrix at $t = 0$.

To study spin relaxation of carriers, it is useful to introduce the spin-dependent electrochemical potentials, which deviate from the Fermi level in the presence of spin polarization of carriers. Spin-dependent electrochemical potentials suggest that up- and down-spin carriers are distinguishable and can reach their own quasi-equilibrium states, which are justified when the spin lifetime is long. While the (spin-polarized) carrier density and the (spin-polarized) electrochemical potential are closely related, the electrochemical varies much slower in space than the carrier density, which can fluctuate at the small scale of the Debye length, and is therefore advantageous in describing transport. For the Boltzmann distribution,[34]

$$\rho_i^q = \rho_i^0 \mu_i^q / k_B T, \tag{3.35}$$

where k_B is the Boltzmann constant and T the temperature, and μ_i^q is the splitting in spin-polarized electrochemical potentials along the q-axis. As the spin-polarized chemical density, the spin-polarized electrochemical potential can be written as $\hat{\mu}_i = \mu_i^0 \hat{1} + \sum_q \hat{\sigma}_q \mu_i^q$. The matrix form is necessary when a common spin quantization axis in a system cannot be defined, e.g., when spin precession occurs. As a result, Eq. (3.34) can be rewritten as

$$\begin{aligned} \sum_i \rho_i^0 \frac{d\mu_i^q}{dt} &= \frac{2}{\hbar^2} \sum_{ijrqs\alpha\beta} (\alpha|\hat{\sigma}_q|\beta)(\beta|[[\hat{\sigma}_r, \hat{\sigma}_q], \hat{\sigma}_s]|\alpha) \\ &\times L_{qq}^{ij}(\omega) \rho_j^0 \mu_j^s, \end{aligned} \tag{3.36}$$

where α and β represent spin and $\alpha(\beta) = \uparrow (\downarrow)$, $\hbar\omega$ is the energy difference between sites i and j, and

$$L_{qq}^{ij}(\omega) = \int_0^{+\infty} \overline{V_{ji}^q(t) V_{ij}^q(t+\tau)} e^{-i\omega\tau} d\tau. \tag{3.37}$$

The spin-conserving hopping rate can be also expressed in terms of the temporal correlation function,[13]

$$w_{ij}^0 = \frac{1}{\hbar^2}\int_0^{+\infty} \overline{V_0^{ji}(t+\tau) V_0^{ij}(t)} e^{i(E_j - E_i)\tau/\hbar} d\tau, \tag{3.38}$$

and $L_{qq}^{ij}(\omega) = \chi^2 w_{ij}^0$ according to Eq. (3.10). Equation (3.36) is then reduced to

$$\rho_i^0 \frac{d\mu_i^q}{dt} = \sum_j [(1-\chi^2)\rho_j^0 w_{ji}^0 \mu_j^q - (1+\chi^2)\rho_i^0 w_{ij}^0 \mu_i^q]. \tag{3.39}$$

In the absence of electric field, the detailed balance requires $\rho_i^0 w_{ij}^0 = \rho_j^0 w_{ji}^0$, and the above equation is further simplified,

$$\frac{\rho_i^0}{k_B T}\frac{d\mu_i^q}{dt} = \sum_j Z_{ij}^{-1}[(1-\chi^2)\mu_j^q - (1+\chi^2)\mu_i^q], \tag{3.40}$$

where $Z_{ij}^{-1} = \rho_i^0 w_{ij}^0 / k_B T = \rho_j^0 w_{ji}^0 / k_B T$.

To determine the carrier spin relaxation time, we track the time evolution of a spatially homogeneous spin polarization, μ^q. In this case, Eq. (3.40) reads

$$\frac{d\mu^q}{dt} = -\frac{2\chi^2 \mu^q k_B T \sum_{ij} Z_{ij}^{-1}}{\sum_i \rho_i^0} \equiv -\mu^q / T_1, \tag{3.41}$$

and the spin relaxation rate is

$$\frac{1}{T_1} = \frac{8\gamma^2}{3}\frac{k_B T \sum_{ij} Z_{ij}^{-1}}{\sum_i \rho_i^0}. \tag{3.42}$$

Since, fundamentally, carrier spin relaxation should be closely related to carrier's motion, we establish the relation between the spin lifetime and electrical transport properties in organics. According to the Einstein relation, the diffusion constant D and the mobility ν are related by $\nu = eD/k_B T$. Using the Kubo formula for mobility, the diffusion constant of the system is expressed as[35]

$$D = \frac{k_B T}{3}\sum_q \int_0^\infty dt e^{-\delta t}\int_0^{1/k_B T} d\lambda \langle v_q(-i\lambda) v_q(t)\rangle, \tag{3.43}$$

where $\langle\ \rangle$ denotes the average with the weighting functional $\exp[-(H_0 + H_{SO})/k_B T]$, and $\delta = 0^+$ is introduced to ensure the above expression is convergent as $t \to \infty$. The velocity operator $\boldsymbol{v}$ can be obtained from

$$\boldsymbol{v} = \frac{i}{\hbar}[H, \boldsymbol{R}] \equiv \frac{i}{\hbar}[H_0 + H_{SO} + V, \boldsymbol{R}], \tag{3.44}$$

where $\boldsymbol{R} = \sum_i \boldsymbol{R}_i a_i^\dagger a_i$ is the polaron position operator. For localized polarons in the hopping regime, the velocity operator has nonzero matrix elements only between different sites,

$$\langle j|\boldsymbol{v}|i\rangle = \frac{i}{\hbar}\langle j|V|i\rangle(\boldsymbol{R}_j - \boldsymbol{R}_i). \tag{3.45}$$

Here we neglect all spin-flip terms because they are proportional to the small spin admixture parameter γ. The DC diffusion constant, in the limit of $|E_i - E_j| \ll \hbar/\tau_c$

$$D = \frac{1}{3}\frac{1}{Z}\sum_i e^{-E_i/k_BT}\sum_j\sum_q |V_{ij}^0|^2 R_{ij}^2 \rho_{ij}(E), \quad (3.46)$$

where $Z = \sum_i e^{-E_i/k_BT}$. After averaging over the molecular orientations, Eq. (3.46) reduces to

$$D = \frac{1}{6}\frac{\sum_i \rho_i^0 w_{ij}^0 \bar{R}^2}{\sum_i \rho_i^0}, \quad (3.47)$$

where $\bar{R}$ is the average hopping distance. Comparing Eq. (3.47) with Eq. (3.42), we obtain

$$T_1^{-1} = T_2^{-1} = \frac{8}{3}\gamma^2\frac{\sum_i \rho_i^0 w_{ij}^0}{\sum_i \rho_i^0} = \frac{16\gamma^2 D}{\bar{R}^2}. \quad (3.48)$$

According to Eq. (3.48) and the Einstein relation, $T_1 \propto D^{-1} \propto \nu^{-1}$, i.e., the higher mobility the shorter spin relaxation time. It is interesting to compare the above theory with the EY mechanism in crystalline semiconductors. While the EY mechanism is is also due to the SOC-induced spin mixing, the disorientation of spin occurs in the process of momentum scattering instead of carrier hopping. Consequently the spin relaxation rate $1/T_1$ in the EY mechanism is proportional to the momentum scattering rate $1/\tau_p$ (τ_p is the carrier mean free time). Since in a crystal, the carrier mobility can be written as $\nu = e\tau_p/m^*$ (m^* is the carrier's effective mass), the experimental signature of the EY mechanism in crystalline semiconductors is $T_1 \propto \nu$, i.e., the spin relaxation time is longer for a higher mobility.[7] The opposite mobility dependences of the spin lifetime in crystalline semiconductors and in disordered organic solids are due to the distinct carrier transport mechanisms: band conduction in the former, where phonon scattering *reduces* τ_p and carrier mobility, and hopping conduction in the latter, where phonons facilitate electron hopping and *enhances* carrier mobility.

Based on the above discussion, we expect that the spin lifetime will decrease with temperature as the mobility generally increases with temperature in the hopping regime. The magnetic field effect should be weak as it does not affect the spin mixing due to the SOC.

IV. SPIN DIFFUSION LENGTH

The spin diffusion length, which measures how far a spin imbalance can traverse in the material, plays a central role in spintronics because it limits the channel length of spintronic devices. To determine the spin diffusion length in organics, we examine the spatial dependence of spin polarization in a steady state ($d\mu_i^q/dt = 0$) from Eq. (3.40). By expanding μ_i^q over distance,

$$\mu^q(\boldsymbol{r}_j) = \mu^q(\boldsymbol{r}_i) + \boldsymbol{R}_{ji}\cdot\nabla\mu^q(\boldsymbol{r}_i) + \frac{1}{2}\boldsymbol{R}_{ji}\boldsymbol{R}_{ji} : \nabla\nabla\mu^q(\boldsymbol{r}_i), \quad (4.1)$$

where $\boldsymbol{R}_{ji} = \boldsymbol{R}_j - \boldsymbol{R}_i$, and summing over i, Eq. (3.40) is reduced to

$$\sum_{ij} Z_{ij}^{-1}[-2\chi^2\mu^q(\boldsymbol{r}_j) + \frac{1}{6}R_{ij}^2\nabla^2\mu^q(\boldsymbol{r}_j)] = 0. \quad (4.2)$$

Comparing it with the definition of spin diffusion length L_s,

$$(\nabla^2 - L_s^{-2})\mu^q(\boldsymbol{r}) = 0, \quad (4.3)$$

we find

$$L_s = \frac{1}{4\gamma}\sqrt{\frac{\sum_{ij} Z_{ij}^{-1}R_{ij}^2}{\sum_{ij} Z_{ij}^{-1}}} \equiv \frac{1}{4\gamma}\bar{R}. \quad (4.4)$$

This remarkably simple expression suggests that the spin diffusion length in organic solids is essentially determined by the spin admixture and average hopping distance and does not depend on the carrier mobility. Hence in contrast to the common assumption, the spin diffusion length cannot be significantly increased by improving the carrier mobility in organics if the SOC is the main source of spin relaxation.

Recently spin diffusion lengths were directly measured by muon spin rotation in Alq_3 at low temperatures[15] and by spin polarized two-photon photoemission in CuPc at room temperature.[16] These experiments provide valuable information on spin transport and allow a direct comparison with theory. Here we analyze the two systems using the above theory.

A. Spin diffusion in Alq_3

According to the muon experiment, the spin diffusion length decreases as temperature increases and levels off when the temperature is above 80 K, as shown in Fig. 4. Here we show that the experimental data can be consistently explained by our theory after noticing that polarons can take advantage of variable-range hopping (VRH) at low temperatures.

In disordered systems, VRH is frequently observed at low temperatures.[36] The origin of VRH is that the hopping probability depends on two factors: the electron wave-function overlap, which decays exponentially over the hopping distance, and the energy difference between hopping sites, which tends to be small when the hopping distance is large. The competition between the two factors results in a temperature-dependent average hopping distance. The signature of the VRH is that the conductivity of the material has a temperature dependence of $\exp -(T/T_0)^{1/4}$. When the Coulomb interaction is important, the temperature dependence becomes $\exp -(T/T_0)^{1/2}$.[37] The average hopping distance is $\bar{R} \sim T^{-1/4}$,[36] or $\bar{R} \sim T^{-1/2}$ for the strong Coulomb interaction case. The VRH has been observed in organic

solids[38] and biological systems.[40] Thus the experimentally measured spin diffusion length in Alq_3 is consistent with Eq. (4.4) in the VRH regime.

To provide a detailed understanding of spin diffusion in Alq_3, we solve transport equations Eq. (3.40) in a $32\times32\times32$ cubic lattice, where each lattice site represents an Alq_3 molecule. A spin imbalance is injected into the lattice at the edge plane of $x = 0$, and at the other edge plane $x = 31a$ (a is the lattice constant), the spin imbalance is set zero. To avoid possible boundary effects, we artificially increase γ^2 from 0.00107 listed in Table II to 0.0375 and multiply the numerically obtained diffusion length by $(0.0375/0.0107)^{1/2}$ to compare with experiment. The lattice constant is chosen to be 11.6 Å, similar to the size of the Alq_3 molecule. We assume the hopping rate between sites i and j has the following Efros-Shklovskii form,[37]

$$w_{ij}^0 = \nu_0 \exp\Big[-2R_{ij}/\ell - (E_i - E_j - E_C/R_{ij})/2k_BT\Big], \tag{4.5}$$

where E_C is the Coulomb gap, and ℓ is the polaron delocalization length and their values are set $E_C = 0.3$ eV and $\ell = 0.64$ Å^{-1} in the calculations. We assume that the polaron energy fluctuations are negligible compared to the Coulomb gap, $|E_i - E_j| \ll E_C$, and are set zero. In the numerical calculations, we allow polarons to hop between any two sites, and therefore VRH is automatically included in the model. The spin imbalance is found to exponentially decay over distance, $\mu^q(x) \sim e^{-x/L_s}$, and the extracted spin-diffusion length is plotted in Fig. 4. We also show in Fig. 4 the averaged hopping distance $\bar{R}$ defined in Eq. (4.4). We see an excellent agreement between the experiment and theory as well as a close correlation between the hopping distance and spin diffusion length. The leveled spin diffusion length occurs when the hopping distance reaches the lattice constant a, the minimal hopping distance possible, as the temperature increases.

Thus we expect the spin diffusion length in organics should decrease with temperature relatively slowly, following $L_s \sim T^{-1/2}$ or $L_s \sim T^{-1/4}$.

B. Spin diffusion in CuPc

The spin diffusion length in CuPc at room temperature has been measured by the spin-polarized two-photon photoemission. It is found that the polaron mean free path is about 1 nm and the spin diffusion length, or the spin-flip length, is about 10 nm. To explain the experiment, we must examine the hopping among $3d$ orbitals.

CuPc has an electronic configuration of $3d^9$, which is equivalent of one hole in a completely filled $3d$ shell. In the hole representation, the electron or hole polaron occupies $|E''\rangle$ in each molecule and hopping takes place between these states at different sites.

If we denote the hopping matrix element between aligned $3d$ orbitals as V_0, the spin-conserving hopping

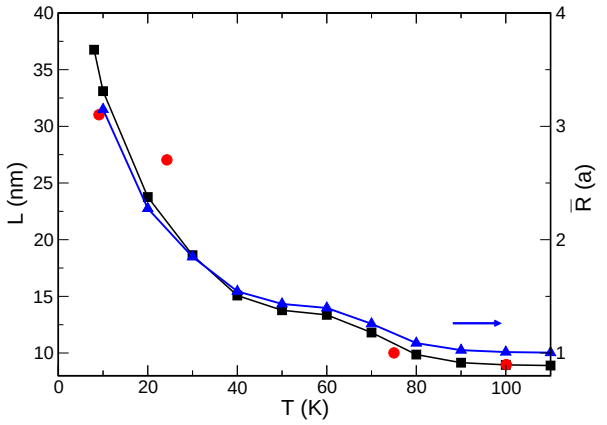

FIG. 4: (color online) Spin diffusion length as a function of temperature in Alq_3. Circles are experimental values and the squares are theoretical values obtained by solving Eq. (3.40) in steady-state on a $32\times32\times32$ lattice with the lattice constant $a = 11.5$ Å. The average hopping distances are represented by triangles.

averaged over random orientations of the molecules is

$$\begin{aligned}\overline{|\langle E''+''|V|E''+'\rangle|^2} &= \overline{|\langle d''_{x^2-y^2}|V|d'_{x^2-y^2}\rangle|^2}\\ &= \frac{1}{4}(\overline{|D^{(2)}_{22}|^2} + \overline{|D^{(2)}_{2-2}|^2} + \overline{|D^{(2)}_{-22}|^2} + \overline{|D^{(2)}_{-2-2}|^2})V_0^2\\ &= \frac{1}{5}V_0^2.\end{aligned} \tag{4.6}$$

Here $D^{(2)}_{mm'}$ is the Wigner D-matrix[33] for $j = 2$ required to transform d_m in one rotation frame to $d_{m'}$ in another and its average over molecular orientations is explained in Appendix C. The spin-flip hopping matrix element can be written as

$$\begin{aligned}\langle E''-''|V|E''+'\rangle &= \frac{\tilde{\xi}_{\rm Cu}}{\Delta_1}\Big(-i\sin\theta'' e^{i\phi''}\langle d''_{x^2-y^2}|V|d'_{xy}\rangle\\ &+ i\sin\theta' e^{i\phi'}\langle d''_{xy}|V|d''_{x^2-y^2}\rangle\Big)\\ &+ \frac{\sqrt{2}}{2}\frac{\xi_{\rm Cu}}{\Delta_2}\Big(\cos^2\frac{\theta''}{2}e^{i\phi''}\langle d''_{x^2-y^2}|V|d''_{xy}\rangle\\ &+ \cos^2\frac{\theta'}{2}e^{i\phi'}\langle 1''|V|d'_{x^2-y^2}\rangle\\ &- \sin^2\frac{\theta''}{2}e^{i\phi''}\langle d'_{x^2-y^2}|V|1''\rangle - \sin^2\frac{\theta'}{2}e^{i\phi'}\langle -1''|V|d''_{x^2-y^2}\rangle\Big),\end{aligned}$$

and the hopping rate, after averaging over molecular orientations, is

$$\overline{|\langle E''-''|V|E''+'\rangle|^2} = \frac{2}{5}\Big[\Big(\frac{\tilde{\xi}_{\rm Cu}}{\Delta_1}\Big)^2 + \frac{1}{2}\Big(\frac{\tilde{\xi}_{\rm Cu}}{\Delta_2}\Big)^2\Big]V_0^2. \tag{4.7}$$

Thus the ratio of the spin-flip hopping to the spin-conserving one is

$$\frac{\overline{|\langle E''-''|V|E''+'\rangle|^2}}{\overline{|\langle E''+''|V|E''+'\rangle|^2}} = \frac{4}{3}\gamma^2. \tag{4.8}$$

Since the mean free path, beyond which the carrier transport is incoherent, in CuPc films is about $l = 1$ nm, which is comparable to the size of the molecule (1.4 nm), we can regard l as the hopping distance and obtain the spin diffusion length,

$$L_s = \frac{\bar{R}}{4\gamma} = \frac{l}{4\gamma} = 9.6 \text{ nm}, \tag{4.9}$$

which is in excellent agreement with experimental value, $L_s = 10$ nm.

Table III summarizes our calculated spin diffusion lengths for different materials, where DO-PPV refers to poly(2,5-dioctyloxy-1,4-phenylenevinylene). We assume that the hopping takes place between nearest neighbors and thus the spin diffusion lengths correspond to their high-temperature values. The average hopping distance is estimated from $\bar{R} = \Omega^{1/3}$, where Ω is the molecular volume in the corresponding molecular crystal based on the X-ray data in literature. Experimentally the spin diffusion length is *directly* measured only in Alq_3 and in CuPc. More frequently, the spin diffusion length in organics is extracted from the magnetoresistance (MR) in organic spin-valve (OSV) structures and involves some uncertainties, depending on the fitting expressions used. These *indirect* measurements yield $L_s = 70$ nm in T_6 at room temperature,[2] 45 nm in Alq_3 at 11K,[3] and 13 nm in rubrene at 0.45 K.[38] The values for T_6 and Alq_3 are in good agreement with the theoretical estimates but the rubrene value is much smaller than what the theory predicts. Apart from the experimental uncertainties, it is possible that the HFI, which is not included in these calculations, is important in rubrene.

We emphasize that a longer spin diffusion does not necessarily translate to a larger MR in an OSV. Experimentally, the measured MR values in OSVs with Alq_3 scatter over a broad range for different electrodes and temperatures.[3,15] Although a consistent picture of the MR in OSVs is not yet available, it is fair to say that the MR may be more sensitive to the spin injection efficiency than the spin diffusion length. In fact, in inorganic systems, spin injection into a metal is generally more efficient than into a semiconductor, although the spin diffusion length in a semiconductor is much longer than in a metal.[1] In general, spin injection depend on many material properties in a device, including magnetizations of the ferromagnets and electrical transport properties of the organic. Since electrical transport in an organic may strongly depend on the material thickness (for example, its resistance increases nonlinearly with the thickness), it is possible that a pronounced MR only appears in an OSV with the channel length much shorter than the spin diffusion length. This may explain the much longer estimated spin diffusion length of C_{60} in Table III than the channel length of C_{60}-based OSVs that show sizable MR.[39]

TABLE III: Spin diffusion lengths of the electron and hole polarons in various organics at room temperature.

Material	hopping distance (Å)	electron (nm)	hole (nm)
benzene	4.9	337	524
Alq_3	14.8	11.2	60
DO-PPV	10.1	491	131
T_6	12.8	47	201
rubrene	14.1	1083	1103
CuPc	10	10	10
PPP	5.9	426	574
C_{60}	20.0	472	437
PTCDIC4F7	11.3	149	70

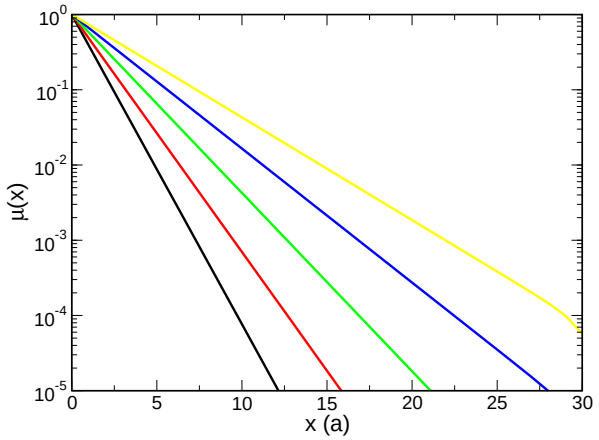

FIG. 5: (color online) Averaged spin imbalance in the y-z plane as a function of x in a $32 \times 32 \times 32$ cubic lattice for different electric fields. The spin imbalance is injected at $x = 0$ and the electric field is along the x-axis. Solid lines, from top to bottom, correspond to $Ea = -0.006$, -0.003, 0, -0.003, and 0.006 V. $T = 110$ K and $\gamma^2 = 0.0375$. Other parameters are the same as in Fig. 4.

V. ELECTRICAL-FIELD EFFECTS ON SPIN DIFFUSION

Most organic materials in spintronic devices are undoped and do not have carriers on their own. All carriers in an organic device are therefore injected from the electrodes. Thus the electric field in organic devices is in general significant. In addition, the MR in OSVs is found to be very sensitive to the bias voltage, suggesting a strong electric-field effect on spin transport. Since the MR in OSVs is pronounced only at relatively low voltages (≤ 1 V),[2,3,15,38,39] we focus on how spin diffusion is affected by a small to moderate electric field.

While the distribution of the carrier density in an organic device structure can be very inhomogeneous, the electrochemical potential varies slowly in space. In fact, in equilibrium, the electrochemical potential (Fermi level) is a constant throughout the device. Similarly,

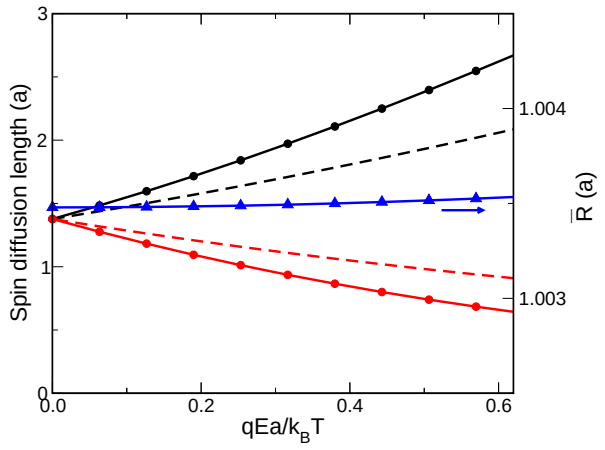

FIG. 6: (color online) Spin diffusion length as a function of electric field. Black and red (gray) circles are upstream and downstream spin diffusion lengths extracted from numerical solutions of Eq. (5.2). Black and red (gray) dashed lines plot Eqs. (5.5) and (5.6). Blue triangles are the average hopping distance as a function of electric field. Other parameters are the same as in Fig. 5.

the splitting in the spin polarized electrochemical potentials, which describes spin imbalance of carriers, does not change as significantly as the spin-polarized carrier density in device structures and is largely independent of charge transport, which is controlled by the spin-independent electrochemical potential μ_0 introduced in Sec. III.D. Thus the effect of electric field can be conveniently studied by Eq. (3.39) without explicitly considering the charge transport. An electric field tilts the polaron energy difference between two sites, and for electron polarons, the hopping probability from site i to site j in the presence of an electric field $\boldsymbol{E}$ can be written as

$$\tilde{w}^0_{ij} = w^0_{ij} e^{e\boldsymbol{E}\cdot(\boldsymbol{R}_i-\boldsymbol{R}_j)/2k_BT} \equiv w^0_{ij} e^{e\boldsymbol{E}\cdot\boldsymbol{R}_{ij}/2k_BT}, \quad (5.1)$$

where e is the absolute value of the electron charge. The presence of an electric field renders $\rho^0_i \tilde{w}^0_{ij} \neq \rho^0_j \tilde{w}^0_{ji}$, and in the steady-state, Eq. (3.39) becomes

$$0 = \sum_j [(1-\chi^2)\rho^0_j \tilde{w}^0_{ji} \mu^q_j - (1+\chi^2)\rho^0_i \tilde{w}^0_{ij} \mu^q_i]. \quad (5.2)$$

By expanding the exponential in Eq. (5.1) for the field with $eE\bar{R}/k_BT < 1$ and using Eq. (4.1), the spin imbalance satisfies the following equation,

$$0 = \sum_j [-2\chi^2 \mu^q_i - \frac{qR^2_{ij}}{6k_BT}\boldsymbol{E}\cdot\nabla\mu^q_i + \frac{1}{6}R^2_{ij}\nabla^2\mu^q_i], \quad (5.3)$$

or, equivalently,

$$\nabla^2\mu^q - \frac{q}{k_BT}\boldsymbol{E}\cdot\nabla\mu^q - 16\gamma^2\frac{\mu^q}{\bar{R}^2} = 0, \quad (5.4)$$

which resembles the spin drift-diffusion equation obtained in inorganic semiconductors. The electric field gives rise to a spin-drift term in Eq. (5.4), which leads to the down- and upstream spin diffusion lengths,

$$\frac{L_d}{a} = \left[-\frac{q|E|a}{2k_BT} + \sqrt{\left(\frac{q|E|a}{2k_BT}\right)^2 + \frac{16\gamma^2a^2}{\bar{R}^2}}\right]^{-1}, \quad (5.5)$$

$$\frac{L_u}{a} = \left[\frac{q|E|a}{2k_BT} + \sqrt{\left(\frac{q|E|a}{2k_BT}\right)^2 + \frac{16\gamma^2a^2}{\bar{R}^2}}\right]^{-1}. \quad (5.6)$$

For a more detailed understanding, we numerically solve Eq. (5.2) using the hopping probability of Eq. (5.1) in the $32\times32\times32$ cubic lattice. The spin imbalance also decays exponentially over the distance with the decay rate strongly depending on the magnitude and direction of the electric field, as shown in Fig. 5. The extracted spin diffusion lengths, shown in Fig. 6, confirm that the presence of electric field results in the upstream and downstream diffusion lengths. The numerical results are similar to the analytical results of Eqs. (5.5) and (5.6), and their quantitative difference is due mainly to the small field approximation used in deriving Eq. (5.3).

The field-dependent spin diffusion is not caused by the change in hopping distance, which is negligible and depends slightly on the absolute value of electric field, as shown in Fig. 6. Rather, it is due to the electric field induced drift. The electric-field effect on spin diffusion suggests that a bias voltage can strongly modify the spin transport behavior and must be included to understand the MR in OSVs.

VI. g FACTOR IN ORGANIC MATERIALS

The SOC also affects the spin resonance frequency of the polaron state and makes the g-factor deviate from the free electron value of $g_e = 2.0023$. Since the g-factor deviation can be measured by ESR, the SOC in individual organics in principle can be characterized by the g-factor deviation. Thus it is also useful to understand the relation between the g-factor deviation and spin admixture γ^2.

The g-factor is defined via the Zeeman energy splitting between up-spin and down-spin states under a given magnetic field, $\boldsymbol{B}$,

$$H_Z = \mu_B \boldsymbol{B}\cdot\mathbf{g}\cdot\boldsymbol{S}, \quad (6.1)$$

where the effective g-factor $\mathbf{g}$ is a tensor. The Zeeman energy contains contribution from both the orbital and spin angular momenta,

$$H_Z = \mu_B \boldsymbol{B}\cdot(\boldsymbol{L} + g_e\boldsymbol{S}). \quad (6.2)$$

By comparing the two Hamiltonians in the eigen-state basis set, the g-factor tensor g_{pq} and its deviation from the free-electron value, $\delta g_{pq} \equiv g_{pq} - g_e\delta_{pq}$, can be obtained.

A. The fictitious atom and molecule

First we evaluate the g-factor change due to the SOC in the fictitious atom introduced in Sec. II.A with its π orbital oriented along (θ,ϕ). The eigenstates of π-electrons, after including the SOC, are $|+'\rangle$ and $|-'\rangle$ in Eqs. (2.8) and (2.9). Note that orbitals p'_q there are defined in the local coordinates of the atom (p'_z is the π orbital), which differ by a rotation from the laboratory coordinates in which Hamiltonian (6.2) is defined. While one can use Eqs. (2.5)-(2.7) to express p'_q in terms of p_q in the laboratory coordinates, a more efficient and elegant way is to use equalities of rotation operators on the angular momentum operators. For example,

$$e^{-i\phi L_z}L_x e^{i\phi L_z} = L_x\cos\phi + L_y\sin\phi, \quad (6.3)$$
$$e^{-i\phi L_z}L_y e^{i\phi L_z} = -L_x\sin\phi + L_y\cos\phi. \quad (6.4)$$

This approach becomes particularly useful when dealing with orbitals with a high angular momentum like $3d$ orbitals. The calculated matrix elements of Hamiltonian (6.2) between $|\pm'\rangle$ are

$$\begin{aligned}\mu_B^{-1}\langle+'|H_Z|+'\rangle &= -\mu_B^{-1}\langle-'|H_Z|-'\rangle \\ &= \frac{g_e}{2}B_z + \frac{\xi}{\Delta}(-\sin^2\theta B_z + \sin\theta\cos\theta\cos\phi B_x + \sin\theta\cos\theta\sin\phi), \quad (6.5)\\ \mu_B^{-1}\langle+'|H_Z|-'\rangle &= \mu_B^{-1}\langle-'|H_Z|+'\rangle^* \\ &= \frac{g_e}{2}(B_x - iB_y) + \frac{\xi}{\Delta}e^{-i\phi}[\sin\theta\cos\theta B_z - (i\sin\phi + \cos^2\theta\cos\phi)B_x + (i\cos\phi - \cos^2\theta\sin\phi)B_y]. \quad (6.6)\end{aligned}$$

Comparing the above matrix with Hamiltonian (6.1) in the 2×2 spin space,

$$H_Z = \frac{\mu_B}{2}\sum_{pq} B_p g_{pq}\hat{\sigma}_q \quad (6.7)$$

we obtain all components of the g-factor tensor,

$$g_{xx} = g_e - \frac{2\xi}{\Delta}(\cos^2\theta\cos^2\phi + \sin^2\phi), \quad (6.8)$$
$$g_{yy} = g_e - \frac{2\xi}{\Delta}(\cos^2\theta\sin^2\phi + \cos^2\phi), \quad (6.9)$$
$$g_{zz} = g_e - \frac{2\xi}{\Delta}\sin^2\theta, \quad (6.10)$$
$$g_{xy} = g_{yx} = \frac{2\xi}{\Delta}(1-\cos^2\theta)\sin\phi\cos\phi, \quad (6.11)$$
$$g_{xz} = g_{zx} = \frac{2\xi}{\Delta}\sin\theta\cos\theta\cos\phi, \quad (6.12)$$
$$g_{yz} = g_{zy} = \frac{2\xi}{\Delta}\sin\theta\cos\theta\sin\phi. \quad (6.13)$$

In disordered organic solids, the molecules are oriented randomly, and therefore the experimentally measured g-factor from ESR should be an ensemble average over different molecular orientations. Since the direction of an applied magnetic field in ESR is well defined, say along the z-axis, the measured g-factor deviation would be $\overline{\delta g_{zz}}$. From Eqs. (6.7)-(6.9), the g-factor deviations, after the orientation average, are

$$\overline{\delta g_{zz}} = \overline{\delta g_{xx}} = \overline{\delta g_{yy}} = -\frac{4\xi}{3\Delta}. \quad (6.14)$$

It is desirable to obtain the averaged g-factor deviation from an invariant quantity of the g-factor tensor, which would allow a theoretical determination of the averaged g-factor deviation by studying a molecule with a single orientation. We find two invariances from Eqs. (6.7)-(6.12),

$$\overline{\delta g} \equiv \frac{1}{3}(\delta g_{xx} + \delta g_{yy} + \delta g_{zz}) = -\frac{4\xi}{3\Delta}, \quad (6.15)$$
$$\overline{|\delta g|} \equiv \sqrt{\sum_{pq} g_{pq}^2} = \frac{2\sqrt{2}\xi}{\Delta}, \quad (6.16)$$

which are independent to the molecular orientation with the ratio of their magnitudes being $\sqrt{2}/3$. In particular, $\overline{\delta g}$ is identical to the ensemble averaged $\overline{\delta g_{qq}}$.

We see that both $\overline{\delta g}$ and $\overline{|\delta g|}$ are proportional to the spin admixture γ introduced earlier. Thus in principle they can be used to measure the SOC. However, by inspecting Hamiltonian (6.2), it is clear that the g-factor deviation comes from mixing between different *orbitals*. It does not include contribution from the spin mixing within a same orbital and therefore may underestimate the spin mixing effect. This is readily seen in the molecule consisting two fictitious atoms studied in Sec. II.D. For the eigenstates of the two-atom molecule, $|\tilde{\pm}\rangle$ in Eq. (2.39), the matrix elements of the Zeeman energy, to the first order of ξ/Δ, is

$$\langle\tilde{\pm}|\boldsymbol{L}+g_e\boldsymbol{S}|\tilde{\pm}\rangle = \frac{1}{2}(\langle\pm'|\boldsymbol{l}_1+g_e\boldsymbol{s}_1|\pm'\rangle+\langle\pm''|\boldsymbol{l}_2+g_e\boldsymbol{s}_2|\pm''\rangle). \quad (6.17)$$

Equation (6.16) suggests that the g-factor deviation $\overline{\delta g}$ in this molecule would be the same as that in an isolated atom. The large spin mixing of the eigenstate Eq. (2.39) will not be reflected in the g-factor deviation, because it occurs mainly within a same orbital. Therefore the

g-factor deviation is not well suited to characterize the spin mixing in organics.

B. CuPc

The polaron in CuPc occupies the $d_{x^2-y^2}$ (E'') state, which mixes with d_{xy} and d_{zx} and d_{yz} via the SOC, as expressed in Eqs. (2.29)-(2.30). The matrix elements of Hamiltonian (6.2) in the space spanned by the eigenstates $|E''\pm\rangle$ are

$$\begin{aligned}
&\mu_B^{-1}\langle E''+|H_Z|E''+\rangle = -\mu_B^{-1}\langle E''-|H_Z|E''-\rangle \\
&= \frac{g_e}{2}B_z + \Big(\frac{4\tilde{\xi}_{\rm Cu}}{\Delta_1}\cos^2\theta + \frac{\tilde{\xi}_{\rm Cu}}{\Delta_2}\sin^2\theta\Big)B_z \\
&+ \Big(\frac{4\tilde{\xi}_{\rm Cu}}{\Delta_1} - \frac{\tilde{\xi}_{\rm Cu}}{\Delta_2}\Big)\sin\theta\cos\theta\cos\phi B_x \\
&+ \Big(\frac{4\tilde{\xi}_{\rm Cu}}{\Delta_1} - \frac{\tilde{\xi}_{\rm Cu}}{\Delta_2}\Big)\sin\theta\cos\theta\sin\phi B_y, \qquad (6.18)\\
&\mu_B^{-1}\langle E''+|H_Z|E''-\rangle = \mu_B^{-1}\langle E''-|H_Z|E''+\rangle^* \\
&= \frac{g_e}{2}(B_x - iB_y) + e^{-i\phi}\Big(\frac{4\tilde{\xi}_{\rm Cu}}{\Delta_1} - \frac{\tilde{\xi}_{\rm Cu}}{\Delta_2}\Big)\sin\theta\cos\theta B_z \\
&+ e^{-i\phi}\Big[\frac{4\tilde{\xi}_{\rm Cu}}{\Delta_1}\sin^2\theta\cos\phi + \frac{\tilde{\xi}_{\rm Cu}}{\Delta_2}(\cos^2\theta\cos\phi + i\sin\phi)\Big]B_x \\
&+ e^{-i\phi}\Big[\frac{4\tilde{\xi}_{\rm Cu}}{\Delta_1}\sin^2\theta\sin\phi \\
&+ \frac{\tilde{\xi}_{\rm Cu}}{\Delta_2}(\cos^2\theta\sin\phi - i\cos\phi)\Big]B_y. \qquad (6.19)
\end{aligned}$$

We obtain the g-factor deviation due to the SOC,

$$\begin{aligned}
\delta g_{zz} &= \frac{8\tilde{\xi}_{\rm Cu}}{\Delta_1}\cos^2\theta + \frac{2\tilde{\xi}_{\rm Cu}}{\Delta_2}\sin^2\theta, \qquad (6.20)\\
\delta g_{xx} &= \frac{8\tilde{\xi}_{\rm Cu}}{\Delta_1}\sin^2\theta\cos^2\phi \\
&+ \frac{2\tilde{\xi}_{\rm Cu}}{\Delta_2}(\sin^2\phi + \cos^2\theta\cos^2\phi), \qquad (6.21)\\
\delta g_{yy} &= \frac{8\tilde{\xi}_{\rm Cu}}{\Delta_1}\sin^2\theta\sin^2\phi \\
&+ \frac{2\tilde{\xi}_{\rm Cu}}{\Delta_2}(\cos^2\phi + \cos^2\theta\sin^2\phi), \qquad (6.22)\\
\delta g_{xy} &= \delta g_{yx} \\
&= \Big(\frac{8\tilde{\xi}_{\rm Cu}}{\Delta_1} - \frac{2\tilde{\xi}_{\rm Cu}}{\Delta_2}\Big)\sin^2\theta\sin\phi\cos\phi, \qquad (6.23)\\
\delta g_{xz} &= \delta g_{zx} \\
&= \Big(\frac{8\tilde{\xi}_{\rm Cu}}{\Delta_1} - \frac{2\tilde{\xi}_{\rm Cu}}{\Delta_2}\Big)\sin\theta\cos\theta\cos\phi, \qquad (6.24)\\
\delta g_{yz} &= \delta g_{zy} \\
&= \Big(\frac{8\tilde{\xi}_{\rm Cu}}{\Delta_1} - \frac{2\tilde{\xi}_{\rm Cu}}{\Delta_2}\Big)\sin\theta\cos\theta\sin\phi. \qquad (6.25)
\end{aligned}$$

Again $\overline{\delta g}$ and $\overline{|\delta g|}$ defined earlier are invariant with respect of any orientation change,

$$\begin{aligned}
\overline{\delta g} &= \frac{8\tilde{\xi}_{\rm Cu}}{3\Delta_1} + \frac{4\tilde{\xi}_{\rm Cu}}{3\Delta_2}, \qquad (6.26)\\
\overline{|\delta g|} &= \sqrt{\Big(\frac{8\tilde{\xi}_{\rm Cu}}{\Delta_1}\Big)^2 + 2\Big(\frac{2\tilde{\xi}_{\rm Cu}}{\Delta_2}\Big)^2}. \qquad (6.27)
\end{aligned}$$

In crystalline CuPc, when the magnetic field is along the normal of the molecular plane, the g-factor change is

$$\delta g_{zz} = \frac{8\xi_{\rm Cu}}{\Delta_1}. \qquad (6.28)$$

When the magnetic field is in the molecular plane, the g-factor change is

$$\delta g_{xx} = \delta g_{yy} = \frac{2\xi_{\rm Cu}}{\Delta_2}. \qquad (6.29)$$

The experimental values are $\delta g_{zz} = 0.164$ and $\delta g_{xx} = 0.05$.[30]

For disordered CuPc films, the averaged g-factor deviations are

$$\overline{\delta g_{zz}} = \overline{\delta g_{xx}} = \overline{\delta g_{yy}} = \overline{\delta g} \simeq 0.088, \qquad (6.30)$$

and $\overline{|\delta g|} \simeq 0.174$.

C. Real organic materials

Using the polaron eigenstates from first-rinciples, Eqs. (2.19) and (2.20), we can calculate the g-factor deviation in representative organics via

$$\delta g_{pq} = -2\sum_{k\neq 0}\frac{\langle\psi_0|\sum_i \xi_i l_{ip}|\psi_k\rangle\langle\psi_k|\sum_j l_{jp}|\psi_0\rangle}{E_k - E_0}, \qquad (6.31)$$

and determine $\overline{\delta g}$ and $\overline{|\delta g|}$.

To test this approach, we first examine δg_{pq} for the electron and hole polaron states in benzene as a function of the molecular orientation θ and display the results in Fig. 7. It is shows that while δg_{qq} depends on the molecular orientation, both $\overline{\delta g}$ and $\overline{|\delta g|}$ are independent of θ and the ratio of their magnitudes is close to $\sqrt{2}/3$ as predicted from Eqs. (6.15) and (6.16). Thus one can reliably estimate the g-factor deviation in a disordered organic material from first-principles calculations.

We also study the g-factor deviation as a function of torsion angle in a twisted biphenyl. We see from Fig. 8 that the averaged $\overline{\delta g}$ is virtually independent of the torsion angle θ except at the angle where the singularity in SOC takes place. The overall change in δg_{qq} over the entire range of θ is very small compared to the change in γ^2, as suggested in Eq. (6.17).

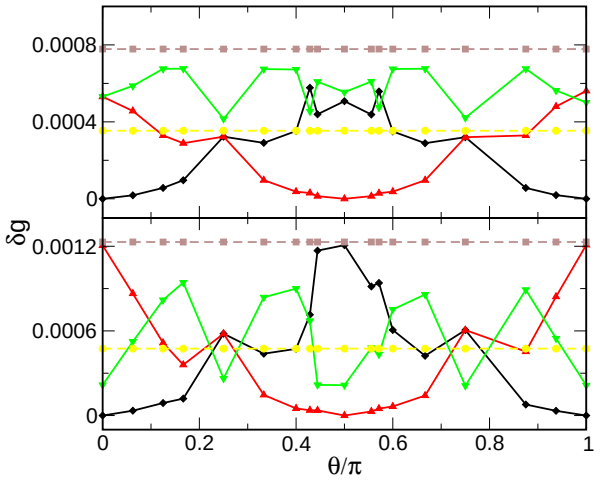

FIG. 7: (color online) g-factor deviation as a function of θ for the electron (upper panel) and hole (lower panel) polarons in benzene. θ is defined as in Fig. 1. Diamonds, up-triangles, and down-triagngles correspond to δg_{zz}, δg_{xx}, and δg_{yy}. Circles and squares represent $\overline{\delta g}$ and $\overline{|\delta g|}$, respectively.

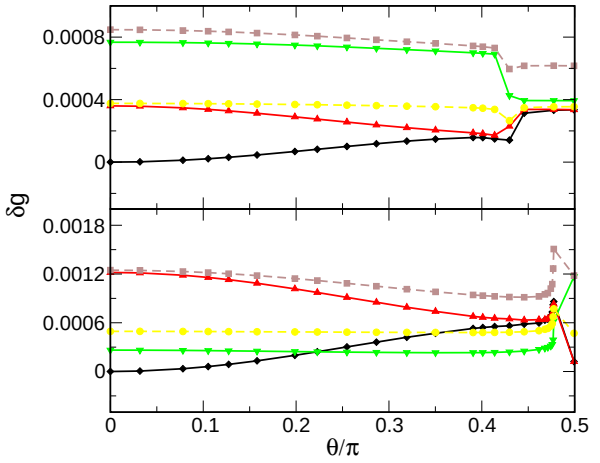

FIG. 8: (color online) g-factor as a function of the torsion angle in twisted biphenyl for the electron (upper panel) and hole (lower panel) polarons. Diamonds, up-triangles, and down-triagngles correspond to δg_{zz}, δg_{xx}, and δg_{yy}. Circles and squares represent $\overline{\delta g}$ and $\overline{|\delta g|}$, respectively.

TABLE IV: g-factors deviation $\overline{\delta g}$ and $\overline{|\delta g|}$ for the electron and hole polarons in various organics. The experimental values are for organics in the form of disordered films.

Material	electron $\overline{\delta g}$ ($\overline{\|\delta g\|}$)	exp $(g-g_e)$	hole $\overline{\delta g}$ ($\overline{\|\delta g\|}$)	exp $(g-g_e)$
benzene	0.00035 (0.00078)	0.0005[41]	0.0005 (0.0012)	0.0002[42]
Alq_3	0.00075 (0.00347)	0.0009[43]	0.0017 (0.0032)	0.0019[43]
MEH-PPV	0.00046 (0.00100)	0.0005[44]	0.0013 (0.0036)	
T_6	0.0026 (0.0057)	0.006[45]	0.00078 (0.00174)	0.0008[46]
PANI	0.00039 (0.00086)		0.00065 (0.0014)	
PPP	0.00044 (0.00098)		0.00045 (0.0011)	
C_{60}	0.00041 (0.00074)	-0.00098[47]	0.00043 (0.00099)	0.0003[48]
rubrene	0.00045 (0.00093)		0.00048 (0.00096)	0.0034[49]
CuPc	0.088 (0.174)		0.088 (0.174)	
PTCDIC4F7	0.0013 (0.0025)		0.00015 (0.0010)	
PPy	0.00036 (0.00077)		0.00043 (0.0010)	

We then carry out first-principles calculations on real organic molecules. The theoretical values of the *disordered* organics and the corresponding experimental values in literature are listed in Table IV. For Alq_3, the obtained g-factor deviation is an average over the HOMO and HOMO$\pm$1 levels for the electron (hole) polaron because the two levels are almost degenerate in energy. The agreement between theory and experiment is overall good with a relative large discrepancy in rubrene than in other materials. The agreement for Alq_3 is particularly encouraging, for the experimental data of Alq_3 are measured in device structures under working conditions.[43] The g-factor changes due to the SOC in organics are generally small, and similar in amplitude except those involving transition metal ions like Cu, where the g-factor deviation is large. It is worth pointing out that the g-factor deviation in Alq_3 is minute compared to its large spin admixture γ^2. This contrast confirms that g-factor underestimates the SOC and therefore is not a good measure of the spin mixing in π-conjugated organics.

VII. SUMMARY

We present a comprehensive study of the SOC in π-conjugated organic materials and its effects on the spin relaxation time, spin diffusion length, and g-factor. To adequately describe the SOC in π-conjugated organics, one must explicitly include σ orbitals in addition to π orbitals. The major effect of the SOC in π-conjugated organics is that it mixes up- and down-spin states, and in the context of spintronics, can be characterized by an admixture parameter in the electron and hole polaron states. The admixture parameters in individual organics can be systematically evaluated from first-principles calculations. Among commonly used π-conjugated organics for spintronic application, the spin admixture parameters can differ by orders of magnitude just like in inorganic materials, indicating that caution must be taken when making general statements on the SOC in organics. Molecular geometry fluctuations, which depend on sample preparation, are found to have a strong effect on the spin mixing. This may explain that many spin-dependent experiments in organic materials are not always reproducible by different groups.

The spin mixing due to the SOC effects spin flips as polarons hop from one molecule to another, giving rise to spin relaxation and diffusion. Thus, in disordered organic solids, the spin lifetime would become longer if the carrier mobility is reduced, which is opposite to the EY spin relaxation mechanism in crystalline semiconductors and metals, where the spin lifetime is proportional to the materials mobility, although the EY mechanism also originates from the SOC-induced spin mixing. Another interesting finding is that the spin diffusion length in organics is largely independent of the carrier mobility and essentially controlled by the spin admixture parameter, suggesting that the spin diffusion length cannot be greatly enhanced by improving the carrier mobility.

An electric field can significantly affect spin transport in the hopping regime, leading to upstream and downstream spin diffusion lengths. This effect can be used to control spin transport in organic spintronic devices and may be responsible to the ubiquitous strong bias dependence of MR observed in OSVs.

The presence of SOC modifies the g-factor of the polaron states from its free-electron value. The g-factor deviation in organics, however, includes only the spin mixing at different orbitals and therefore tends to underestimate the SOC in organics. In particular, the g-factor deviation is not sensitive to the molecular geometry fluctuations, which mainly affect the spin mixing within a same orbital.

The SOCs in Alq_3 and in CuPc are particularly strong, due to the orthogonal arrangement of the three ligands in the former and Cu $3d$ orbitals in the latter. The spin diffusion lengths in these systems are directly measured by muon spin rotations for Alq_3 and spin-polarized two-photon photoemission for CuPc. Both experiments are quantitatively explained by the SOC-induced spin diffusion.

The other important interaction that influences elec-

tron spins in organics is the HFI. The relative importance of the SOC and HFI in organics may vary from material to material, as indicated by the presence and absence of the isotope effect in various organics. A quantitative study of the HFI and its effect on spin-dependent properties in organics would help understand the relative importance of SOC and HFI in individual organic materials and design organic spintronic structures exploiting these interactions.

Acknowledgments

The author is grateful to D. L. Smith and C. F. O. Graeff for helpful discussions. This work was supported by SRI internal funds and by the Office of Basic Energy Sciences, Department of Energy, under Grant No. DE-FG02-06ER46325.

Appendix A: Quasi up- and down-spin states

Here we show that $|+'\rangle$ in Eq. (2.8) has the maximal expectation value of the spin operator $\hat{\sigma}_z$. An arbitrary linear combination of $|+'\rangle$ and $|-'\rangle$ can be generally written as

$$|\theta\rangle = \cos\frac{\theta}{2}|+'\rangle + \sin\frac{\theta}{2}e^{-i\phi}|-'\rangle, \tag{A1}$$

and the spin expectation value is

$$p_\theta \equiv \langle\theta|\hat{\sigma}_z|\theta\rangle = \cos\theta\Big(1-\frac{\xi^2}{2\Delta^2}\cos^2\theta_1\Big) + \sin\theta\cos(\phi_1-\phi)\Big(-\frac{\xi^2}{2\Delta^2}\sin\theta_1\cos\theta_1\Big), \tag{A2}$$

where we have used the matrix elements

$$\langle+'|\hat{\sigma}_z|-'\rangle = \langle-'|\hat{\sigma}_z|+'\rangle^* = -\frac{\xi^2}{2\Delta^2}\sin\theta_1\cos\theta_1 e^{i\phi_1}. \tag{A3}$$

To find the maximum of p_θ, we determine θ and ϕ by solving $\partial p_\theta/\partial\phi = \partial p_\theta/\partial\theta = 0$. We obtain

$$\phi = \phi_1, \quad \tan\theta = \frac{-\frac{\xi^2}{2\Delta^2}\sin\theta_1\cos\theta_1}{1-\frac{\xi^2}{2\Delta^2}\cos^2\theta_1} \simeq -\frac{\xi^2}{2\Delta^2}\sin\theta_1\cos\theta_1, \tag{A4}$$

and the corresponding maximum of p_θ is

$$p_\theta = \cos\theta\Big(1-\frac{\xi^2}{2\Delta^2}\cos^2\theta_1\Big) + \sin\theta\Big(-\frac{\xi^2}{2\Delta^2}\sin\theta_1\cos\theta_1\Big), \tag{A5}$$

which, to the second-order of ξ/Δ, is

$$p_\theta = 1-\frac{\xi^2}{2\Delta^2}\cos^2\theta_1 \equiv p_+. \tag{A6}$$

Similarly, p_- is the largest spin expectation value along the $-z$ direction. Thus one can regard $|+'\rangle$ ($|-'\rangle$) as the quasi up- (down-) spin state.

Appendix B: SU(2) invariance of spin-flip hopping rate

The spin-flip hopping rate is independent of any linear combination, or equivalently, an SU(2) rotation of the eigenstate $|\pm\rangle$. We denote the four eigenstates, $|\pm'\rangle$ and $|\pm''\rangle$, after a rotation, become $(1',2')$ in the first molecule and $(1'',2'')$ in the other. The new hopping matrix becomes

$$\begin{pmatrix} V_{1''1'} & V_{1''2'} \\ V_{2''1'} & V_{2''2'} \end{pmatrix} = \begin{pmatrix} \cos\frac{\theta}{2} & \sin\frac{\theta}{2}e^{i\phi} \\ -\sin\frac{\theta}{2}e^{-i\phi} & \cos\frac{\theta}{2} \end{pmatrix} \begin{pmatrix} V_{+''+'} & V_{+''-'} \\ V_{-''+'} & V_{-''-'} \end{pmatrix} \begin{pmatrix} \cos\frac{\theta}{2} & -\sin\frac{\theta}{2}e^{i\phi} \\ \sin\frac{\theta}{2}e^{-i\phi} & \cos\frac{\theta}{2}. \end{pmatrix} \tag{B1}$$

The new splin-flip hopping probability is

$$\begin{aligned} \overline{|V_{1''2'}|^2} &= \cos^4\frac{\theta}{2}\overline{|V_{+''-'}|^2} + \sin^4\frac{\theta}{2}\overline{|V_{-''+'}|^2} + \sin^2\frac{\theta}{2}\cos^2\frac{\theta}{2}\overline{|V_{+''+'} - V_{-''-'}|^2} \\ &= \overline{|V_{+''-'}|^2}, \end{aligned} \tag{B2}$$

where we have used $\overline{|V_{+''+'} - V_{-''-'}|^2} = 2\overline{|V_{+''-'}|^2} = 4\overline{V_z^2}$.

Appendix C: Average over molecular orientations for $3d$ orbitals

The spin-flip hopping matrix element between $3d$ orbitals of two different sites can be expressed in terms of the rotational matrix $D^{(2)}_{mm'}(\tilde{\alpha},\tilde{\beta},\tilde{\gamma})$, where $\tilde{\alpha}$,$\tilde{\beta}$,$\tilde{\gamma}$ are three Euler angles. For example, the hopping matrix element between d_{z^2} at two different site is

$$\langle d''_{z^2}|V|d'_{z^2}\rangle = D^{(2)}_{00}(\tilde{\alpha},\tilde{\beta},\tilde{\gamma})V_0. \tag{C1}$$

Using the properties of $D^{(2)}_{mm'}$,[33]

$$\overline{D^{(2)*}_{m_1m_2}(\tilde{\alpha},\tilde{\beta},\tilde{\gamma})D^{(2)}_{n_1n_2}(\tilde{\alpha},\tilde{\beta},\tilde{\gamma})} = \delta_{m_1n_1}\delta_{m_2n_2}\overline{|D^{(2)}_{m_1m_2}(\tilde{\alpha},\tilde{\beta},\tilde{\gamma})|^2} = \delta_{m_1n_1}\delta_{m_2n_2}\frac{1}{5}, \tag{C2}$$

we obtain,

$$\overline{|\langle d'_{x^2-y^2}|V|d''_{xy}\rangle|^2} = \frac{V_0^2}{4}\Big(\overline{|D^{(2)}_{22}|^2}+\overline{|D^{(2)}_{2-2}|^2}+\overline{|D^{(2)}_{-22}|^2}+\overline{|D^{(2)}_{-2-2}|^2}\Big) = \frac{1}{5}V_0^2, \tag{C3}$$

$$\overline{|\langle -1'|V|d''_{x^2-y^2}\rangle|^2} = \frac{V_0^2}{2}\Big(\overline{|D^{(2)}_{-12}|^2}+\overline{|D^{(2)}_{-1-2}|^2}\Big) = \frac{1}{5}V_0^2, \tag{C4}$$

$$\overline{|\langle d'_{xy}|V|1''\rangle|^2} = \frac{V_0^2}{2}\Big(\overline{|D^{(2)}_{21}|^2}+\overline{|D^{(2)}_{-21}|^2}\Big) = \frac{1}{5}V_0^2. \tag{C5}$$

[1] A. Fert, Rev. Mod. Phys. **80**, 1517 (2008).
[2] V. Dediu, M. Murgia, F. C. Matacotta, C. Taliani, and S. Barbanera, Solid State Commun. **122**, 181 (2002).
[3] Z. H. Xiong, D. Wu, Z. V. Vardeny, and J. Shi, Nature (London) **427**, 821 (2004).
[4] Editorial, Nature Mater. **8**, 691 (2009).
[5] See, e.g., http://www.nist.gov/physlab/data/asd.cfm.
[6] Z. G. Yu, D. L. Smith, A. Saxena, R. L. Martin, A. R. Bishop, Phys. Rev. Lett. **84**, 721 (2000); Phys. Rev. B **63**, 085202 (2001).
[7] Y. Yafet, Solid State Physics **14**, 1 (1963).
[8] M. I. D'yakonov and V. I. Perel', Sov. Phys. JETP **33**, 1053 (1971).
[9] C. P. Slichter, *Principles of Magnetic Resonance*, 2nd edition (Springer-Verlag, Berlin, 1978).
[10] G. Szulczewski, S. Sanvito, and M. Coey, Nature Mater. **8**, 693 (2009).
[11] V. A. Dediu, L. E. Hueso, I. Bergenti, and C. Taliani, Nature Mater. **8**, 707 (2009).
[12] S. Pramanik, C.-G. Stefanita, S. Patibandla, and S. Bandyopadhyay, Nature Nanotech. **2**, 216 (2007).
[13] Z. G. Yu, Phys. Rev. B **77**, 205439 (2008).
[14] D. R. McCamey, H. A. Seipel, S.-Y. Paik, M. J. Walter, N. J. Borys, J. M. Lupton and C. Boehme, Nature Mater. **7**, 724 (2008).
[15] A. J. Drew, J. Hoppler, L. Schulz, F. L. Pratt, P. Desai, P. Shakya, T. Kreouzis, W. P. Gillin, A. Suter, N. A. Morley, V. K. Malik, A. Dubroka, K.W. Kim, H. Bouyanfif, F. Bourqui, C. Bernhard, R. Scheuermann, G. J. Nieuwenhuys, T. Prokscha, and E. Morenzoni, Nature Mater. **8**, 109 (2009).
[16] M. Cinchetti, K. Heimer, J.-P. Wüstenberg, O. Andreyev, M. Bauer, S. Lach, C. Ziegler, Y. Gao, and M. Aeschlimann, Nature Mater. **8**, 115 (2009).
[17] Z. G. Yu and M. E. Flatté, Phys. Rev. B **66**, 201202 (R) (2002); 235302 (2002).
[18] P. A. Bobbert, W. Wagemans, F. W. A. van Oost, B. Koopmans, and M. Wohlgenannt, Phys. Rev. Lett. **102**, 156604 (2009).
[19] M. I. D'yakonov and V. I. Perel', Sov. Phys. JETP **38**, 177 (1974).
[20] T. D. Nguyen, G. Hukic-Markosian, F. Wang, L. Wojcik, X.-G. Li, E. Ehrenfreund, and Z. V. Vardeny, Nature Mater. **9**, 345 (2010).
[21] N. J. Rolfe, M. Heeney, P. B. Wyatt, A.J. Drew, T. Kreouzis, and W. P. Gillin, Phys. Rev. B **80**, 241201 (R) (2009).
[22] Z. G. Yu, Phys. Rev. Lett. **106**, 106602 (2011).
[23] W. P. Su, J. R. Schrieffer, and A. J. Heeger, Phys. Rev. B **22**, 2099 (1980).
[24] D. S. McClure, J. Chem. Phys. **20**, 682 (1952).
[25] J. Rybicki and M. Wohlgenannt, Phys. Rev. B **79**, 153202 (2009); J. Rybicki, T.D. Nguyen, Y. Sheng, and M. Wohlgenannt, Syn. Met. **160**, 289 (2010).
[26] H. M. McConnell, J. Chem. Phys. **24**, 764 (1956).
[27] E. Pikus and A. N. Titkov, *Optical Orientation* (North Holland, Amsterdam, 1983).
[28] J. M. Soler, E. Artacho, J. D. Gale, A. Garca, J. Junquera, P. Ordejón, and D. Sánchez-Portal, J. Phys.: Condens. Matter **14**, 2745 (2002).
[29] C. J. Ballhausen, *Introduction to Ligand Field Theory* (McGraw-Hill, New York, 1962).
[30] J. F. Gibson, D. J. E. Ingram, and D. Schonland, Discuss. Faraday Soc. **26**, 72 (1958).
[31] These values are obtained from more accurate first-principles calculations and may differ slightly from the values listed in Ref. 22.
[32] R. Schmidt, J. H. Oh, Y.-S. Sun, M. Deppisch, A.-M.

Krause, K. Radacki, H. Braunschweig, M. Könemann, P. Erk, Z. Bao, and F. Würthner, J. Am. Chem. Soc. **131**, 6215 (2009).
[33] See, e.g., L. D. Landau and E. M. Lifshitz, *Quantum Mechanics*, 3rd ed. (Pergamon, Oxford, 1977).
[34] Z. G. Yu, M. A. Berding, and S. Krishnamurthy, Phys. Rev. B **71**, 060408 (R) (2005).
[35] D. Emin, Adv. Phys. **24**, 305 (1975).
[36] N. F. Mott, Adv. Phys. **16**, 49 (1967).
[37] A. L. Efros and B. I. Shklovskii, J. Phys. C.: Solid St. Phys. **8**, L49 (1975).
[38] J. H. Shim, K. V. Raman, Y. J. Park, T. S. Santos, G. X. Miao, B. Satpati, and J. S. Moodera, Phys. Rev. Lett. **100**, 226603 (2008).
[39] M. Gobbi, F. Golmar, R. Llopis, F. Casanova, and L. E. Hueso, Adv. Mat. **23**, 1609 (2011).
[40] Z. G. Yu and X. Song, Phys. Rev. Lett. **86**, 6018 (2001).
[41] B. G. Segal, M. Kaplan, and G. K. Fraenkel, J. Chem. Phys. **43**, 4191 (1965).
[42] T. Komatsu and A. Lund, J. Phys. Chem. **76**, 1727 (1972).
[43] F. A. Castro, G. B. Silva, F. Nüesch, L. Zuppiroli, C. F.O. Graeff, Org. Electron. **8**, 249 (2007).
[44] A. L. Konkin, S. Sensfuss, H.-K. Roth, G. Nazmutdinova, M. Schroedner, M. Al-Ibrahim, D.A.M. Egbe, Syn. met. **148**,199 (2005).
[45] R. Österbacka, C. P. An, X. M. Jiang, and Z. V. Vardeny, Science **287**, 839 (2000).
[46] V. I. Krinichnyi, O. Ya. Grinberg, I. B. Nazarova, G. I. Kozub, L. I. Tkachenko, M. L. Khidekel', and Ya. S. Lebedev, Izvestiya Akademii Nauk SSSR Seriya Khimicheskaya **2**, 467 (1985).
[47] G. L. Closs, P. Gautam, D. Zhang, P. J. Krusic, S. A. Hill, E. Wasserman, J.Phys. Chem. **96**, 5228 (1992).
[48] W. Kempiński, L. Piekara-Sady, E.A. Katz, A.I. Shames, and S. Shtutina, Solid State Commun. **114**, 173 (2000).
[49] M. F. Calhoun, J. Sanchez, D. Olaya, M. E. Gershenson and V. Podzorov, Nature Mater. **7**, 84 (2008).